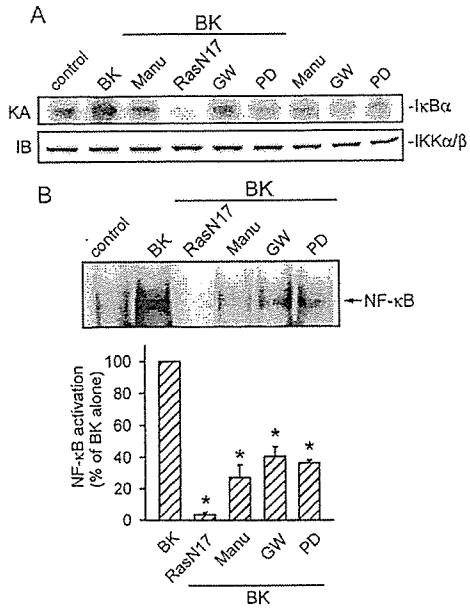

FIGURE 9. Involvement of the Ras/Raf-1/ERK signal pathway in BK-mediated increases in IKK$\alpha\beta$ activity and NF-κB activation in A549 cells. *A*, Cells were pretreated with vehicle, 3 μM manumycin A, 3 nM GW 5074, and 30 μM PD 098059 for 30 min, followed by stimulation with 10 nM BK for another 30 min. Whole cell lysates were prepared, and then immunoprecipitated with Abs specific to IKKα and IKKβ. One set of immunoprecipitates was subjected to the kinase assay (KA) using the GST-IκBα fusion protein as a substrate (*top panel*). The other set of immunoprecipitates was subjected to 10% SDS-PAGE and quantified by immunoblotting (IB) with anti-IKK$\alpha\beta$ Ab (*bottom panel*). Equal amounts of the immunoprecipitated kinase complex present in each kinase assay were confirmed by immunoblotting for IKK$\alpha\beta$. *B*, Cells were transiently transfected with 1 μg of the Ras dominant-negative mutant (RasN17) for 24 h or pretreated with 3 μM manumycin A, 3 nM GW 5074, or 30 μM PD 098059 for 30 min followed by stimulation with 10 nM BK for another 30 min. Nuclear extracts were prepared for determination of NF-κB-specific DNA protein-binding activity by EMSA as described in *Materials and Methods*. The extent of NF-κB activation was quantitated using a densitometer with Image-Pro plus software. Traces represent results from three independent experiments, which are presented as the mean ± SE. *, $p <$ 0.05 as compared with BK treatment.

our results may be of importance in understanding the role of BK in the development of airway inflammatory diseases such as asthma.

COX-2 is an important inducible gene in inflammatory and airway diseases. A number of cytokines are known to induce COX-2 expression through both transcriptional and posttranscriptional mechanisms (13). Previous studies have shown that BK is capable of inducing COX-2 protein expression in airway smooth muscle cells, fibroblasts, and epithelial cells, but the mechanisms involved have not been extensively studied (40). A greater understanding of these mechanisms may provide important information to aid our understanding of how BK acts in airway inflammatory diseases. There are several binding sites for a number of transcription factors including NF-κB, NF-IL-6/C/EBP, AP-1, and cAMP response element in the 5′ region of the *COX-2* gene (41). Recent studies of the human COX-2 promoter have demonstrated that COX-2 induction by several transcription factors occurs in a highly stimulus-specific or cell-specific manner. For example, NF-κB has been shown to control the induced transcription of COX-2 in human lung epithelial cells and airway myocytes (42–44). In foreskin fibroblasts, COX-2 induction by IL-1β used the C/EBP-binding domain (45). In airway smooth muscle cells, BK-induced COX-2 expression was mediated by CCAAT/enhancer protein but not by NF-κB or C/EBP, whereas NF-κB was involved in IL-1β-induced COX-2 expression (46). The results of this study showed that NF-κB activation contributed to BK-induced COX-2 induction in A549 cells, and that the inhibitors of the NF-κB-dependent signaling pathway, including PDTC and TPCK, inhibited BK-induced COX-2 expression. Furthermore, BK induced IKK$\alpha\beta$ activation, IκBα phosphorylation, IκBα degradation, p65 and p50 translocation from the cytosol to the nucleus, and formation of an NF-κB-specific DNA-protein complex, as well as an increase in κB-luciferase activity. Moreover, BK-induced COX-2-luciferase activity was attenuated by transfection with the NF-κB mutant of COX-2 construct. Therefore, NF-κB activation is required to induce COX-2 transcription by BK in A549 cells. The results of this study also showed that Ras, Raf-1, and ERK are involved in NF-κB activation through an increase in IKK$\alpha\beta$ activity. A previous report showed that NF-κB activation is mediated via the Ras-dependent signaling pathway, which induces COX-2 transcriptional gene expression in lung epithelial cells (47). Another previous report also showed that in transformed liver epithelial cells, Ras and Raf lead to constitutive activation of NF-κB through the IKK$\alpha\beta$ complex (48). These pathways may mediate BK effect. As shown in Fig. 9, manumycin A, GW 5074, and PD 098059 blocked BK-induced IKK$\alpha\beta$ activation. In addition, RasN17 and these inhibitors attenuated the BK-mediated formation of the NF-κB-specific DNA-protein complex or COX-2 expression, implying a role in the pathway of NF-κB activation following BK stimulation.

Ras, an oncogenic protein, plays a critical role in inducing COX-2 expression (49, 50). Ras might activate a number of signal pathways, including the Raf-1/MEK/ERK pathway and the PI3K/Akt/NF-κB pathway (26, 51, 52). In murine fibroblasts, activation of the Ras/Raf-1/ERK1/2 signal pathway is required for COX-2 induction (50). In this study, we found that treatment of A549 cells with BK caused subsequent activation of Ras, Raf-1, and ERK, and that manumycin A, GW 5074, and PD 098059 all inhibited BK-induced ERK activation and COX-2 expression. These results suggest that the Ras/Raf-1/ERK signal pathway is very important for the induction of COX-2 caused by BK. This suggestion is further supported by our previous report that lipoteichoic acid induces COX-2 expression through the ERK pathway to induce NF-κB activation in human airway epithelial cells (A549) (53). However, the mechanism by which BK activates Ras has not yet been established. The B2 BK receptor is capable of coupling to several heterotrimeric G proteins depending on the cell type, including G_i/G_o, G_s, G_q, G_{11}, and G_{13} (20, 54–56). After ligand binding to G protein-couple receptor, heterotrimeric G proteins undergo GDP-GTP exchange, whereupon the tightly associated heterotrimeric G protein dissociates into α and β_γ subunits. A constitutively active mutant of $G_{i\alpha 2}$ has been shown to mediate Ras activation (57). A previous report also showed that in HEK293T cells, BK-induced ERK2 activation is dependent on G_i-induced Ras activation (58). However, the exact mechanism by which BK activates Ras needs to be further explored.

Two types of BK receptors have been defined and cloned: B1 and B2 BK receptors (29). We found that the B2 BK receptor antagonist HOE140 potently inhibited BK-induced ERK activation, NF-κB activation, and COX-2 expression, while the B1 BK receptor antagonist (Lys-(Leu^8)des-Arg^9-BK) was inactive. Therefore, BK-stimulated ERK activation, NF-κB activation, and COX-2 expression in human airway epithelial cells are mediated through the B2 BK receptor. Our results are in agreement with the findings that the B2 BK receptor is responsible for BK-stimulated NF-κB activation and IL-1β gene expression in human fibroblasts

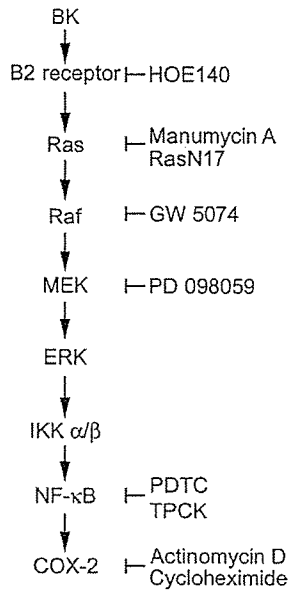

FIGURE 10. Schematic summary of signal transduction by BK induction of COX-2 expression in human airway epithelial cells (A549). BK, acting through the B2 BK receptor, activates the Ras/Raf-1/ERK pathway, which in turn increases IKK$\alpha\beta$ activity, IκBα degradation, and NF-κB activation, and finally induces COX-2 expression in A549 cells.

and epithelial cells (16, 17) and bronchoconstriction in isolated human airways (59, 60).

In summary, we have shown that BK, acting through B2 BK receptors, induces ERK and transcription factor NF-κB activation with a subsequent increase of COX-2 expression in human airway epithelial cells (A549). We have further shown that BK might activate the Ras/Raf-1/ERK pathway, which in turn initiates IKK$\alpha\beta$ and NF-κB activation, and finally induces COX-2 expression in human airway epithelial cells. Fig. 10 is a schematic representation of the signaling pathway of BK-induced COX-2 expression in human airway epithelial cells. These observations provide a novel possible explanation for the critical role of the BK in the transition of acute allergic reactions to chronic airway inflammatory diseases, such as asthma.

Acknowledgments

We thank Dr. Wan-Wan Lin for the kindly gift of pGL2-ELAM-Luc plasmid and pBK-CMV-Lac Z plasmid.

References

1. Proud, D., and A. P. Kaplan. 1988. Kinin formation: mechanisms and role in inflammatory disorders. *Annu. Rev. Immunol. 6:49.*
2. Hall, J. M. 1992. Bradykinin receptors: pharmacological properties and biological roles. *Pharmacol. Ther. 56:131.*
3. Farmer, S. G., D. E. Wilkins, S. A. Meeker, E. A. Seeds, and C. P. Page. 1992. Effects of bradykinin receptor antagonists on antigen-induced respiratory distress, airway hyperresponsiveness and eosinophilia in guinea-pigs. *Br. J. Pharmacol. 107:653.*
4. Tsukagoshi, H., T. Sakamoto, W. Xu, P. J. Barnes, and K. F. Chung. 1994. Effect of interleukin-1β on airway hyperresponsiveness and inflammation in sensitized and nonsensitized Brown-Norway rats. *J. Allergy Clin. Immunol. 93:464.*
5. Pang, L., and A. J. Knox. 1998. Bradykinin stimulates IL-8 production in cultured human airway smooth muscle cells: role of cyclooxygenase products. *J. Immunol. 161:2509.*
6. Vane, J. R., Y. S. Bakhle, and R. M. Botting. 1998. Cyclooxygenases 1 and 2. *Annu. Rev. Pharmacol. Toxicol. 38:97.*
7. Xie, W. L., J. G. Chipman, D. L. Robertson, R. L. Erikson, and D. L. Simmons. 1991. Expression of a mitogen-responsive gene encoding prostaglandin synthase is regulated by mRNA splicing. *Proc. Natl. Acad. Sci. USA 88:2692.*
8. Mitchell, J. A., S. Larkin, and T. J. Williams. 1995. Cyclooxygenase-2: regulation and relevance in inflammation. *Biochem. Pharmacol. 50:1535.*
9. Chiang, L. L., C. T. Kuo, C. H. Wang, T. F. Chen, Y. S. Ho, H. P. Kuo, and C. H. Lin. 2003. Involvement of nuclear factor-κB in lipoteichoic acid-induced cyclooxygenase-2 expression in RAW 264.7 macrophages. *J. Pharm. Pharmacol. 55:115.*
10. Lin, C. H., I. H. Kuan, H. M. Lee, W. S. Lee, J. R. Sheu, Y. S. Ho, C. H. Wang, and H. P. Kuo. 2001. Induction of cyclooxygenase-2 protein by lipoteichoic acid from *Staphylococcus aureus* in human pulmonary epithelial cells: involvement of a nuclear factor-κB-dependent pathway. *Br. J. Pharmacol. 134:543.*
11. Maier, J. A., T. Hla, and T. Maciag. 1990. Cyclooxygenase is an immediate-early gene induced by interleukin-1 in human endothelial cells. *J. Biol. Chem. 265:10805.*
12. Samad, T. A., K. A. Moore, A. Sapirstein, S. Billet, A. Allchorne, S. Poole, J. V. Bonventre, and C. J. Woolf. 2001. Interleukin-1β-mediated induction of Cox-2 in the CNS contributes to inflammatory pain hypersensitivity. *Nature 410:471.*
13. Hinz, B., and K. Brune. 2002. Cyclooxygenase: 2–10 years later. *J. Pharmacol. Exp. Ther. 300:367.*
14. Pang, L., and A. J. Knox. 1997. PGE_2 release by bradykinin in human airway smooth muscle cell: involvement of cyclooxygenase-2 induction. *Am. J. Physiol. 273:L1132.*
15. Tanaka, K., H. Kawasaki, K. Kurata, Y. Aikawa, Y. Tsukamoto, and T. Inaba. 1995. T-614, a novel antirheumatic drug, inhibits both the activity and induction of cyclooxygenase-2 (COX-2) in cultured fibroblasts. *Jpn. J. Pharmacol. 67:305.*
16. Pan, Z. K., B. L. Zuraw, C.-C. Lung, E. R. Prossnitz, D. D. Browning, and R. D. Ye. 1996. Bradykinin stimulates NF-κB activation and interleukin 1β gene expression in cultured human fibroblasts. *J. Clin. Invest. 98:2042.*
17. Pan, Z. K., R. D. Ye, S. C. Christiansen, M. A. Jagels, G. M. Bokoch, and B. L. Zuraw. 1998. Role of the Rho GTPase in bradykinin-stimulated nuclear factor-κB activation and IL-1β gene expression in cultured human epithelial cells. *J. Immunol. 160:3038.*
18. Pan, Z. K., S. C. Christiansen, A. Ptasznik, and B. L. Zuraw. 1999. Requirement of phosphatidylinositol 3-kinase activity for bradykinin stimulation of NF-κB activation in cultured human epithelial cells. *J. Biol. Chem. 274:9918.*
19. Kozma, R., S. Ahmed, A. Best, and L. Lim. 1995. The Ras-related protein Cdc42Hs and bradykinin promote formation of peripheral actin microspikes and filopodia in Swiss 3T3 fibroblasts. *Mol. Cell. Biol. 15:1942.*
20. Ahn, N. G., D. J. Robbins, J. W. Haycock, R. Seger, M. H. Cobb, and E. G. Krebs. 1992. Identification of an activator of the microtubule-associated protein 2 kinases ERK1 and ERK2 in PC12 cells stimulated with nerve growth factor or bradykinin. *J. Neurochem. 59:147.*
21. Mukhin, Y. V., E. A. Garnovsky, M. E. Ullian, and M. N. Garnovskaya. 2003. Bradykinin B2 receptor activates extracellular signal-regulated protein kinase in mIMCD-3 cells via epidermal growth factor receptor transactivation. *J. Pharmacol. Exp. Ther. 304:968.*
22. Campbell, S. L., R. Khosravi-Far, K. L. Rossman, G. J. Clark, and C. J. Der. 1998. Increasing complexity of Ras signaling. *Oncogene 17:1395.*
23. Blaine, S. A., M. Wick, C. Dessev, and R. A. Nemenoff. 2001. Induction of $cPLA_2$ in lung epithelial cells and non-small cell lung cancer is mediated by Sp1 and c-Jun. *J. Biol. Chem. 276:42737.*
24. Marshall, C. J. 1996. Ras effectors. *Curr. Opin. Cell Biol. 8:197.*
25. Zang, M., C. Hayne, and Z. Luo. 2002. Interaction between active Pak1 and Raf-1 is necessary for phosphorylation and activation of Raf-1. *J. Biol. Chem. 277:4395.*
26. Zhang, X. F., J. Settleman, J. M. Kyriakis, E. Takeuchi-Suzuki, S. J. Elledge, M. S. Marshall, J. T. Bruder, U. R. Rapp, and J. Avruch. 1993. Normal and oncogenic $p21^{ras}$ proteins bind to the amino-terminal regulatory domain of c-Raf-1. *Nature 364:308.*
27. Whitmarsh, A. J., and R. J. Davis. 1998. Structural organization of MAP-kinase signaling modules by scaffold proteins in yeast and mammals. *Trends Biochem. Sci. 23:481.*
28. Chen, C. C., J. K. Wang, W. C. Chen, and S. B. Lin. 1998. Protein kinase C η mediates lipopolysaccharide-induced nitric oxide synthase expression in primary astrocytes. *J. Biol. Chem. 273:19424.*
29. Hall, J. M. 1997. Bradykinin receptors. *Gen. Pharmacol. 28:1.*
30. Chen, B. C., C. F. Chou, and W. W. Lin. 1998. Pyrimidinoceptor-mediated potentiation of inducible nitric-oxide synthase induction in J774 macrophages: role of intracellular calcium. *J. Biol. Chem. 273:29754.*
31. Musial, A., and N. T. Eissa. 2001. Inducible nitric-oxide synthase is regulated by the proteasome degradation pathway. *J. Biol. Chem. 276:24268.*
32. Hara, M., K. Akasaka, S. Akinaga, M. Okabe, H. Nakano, R. Gomez, D. Wood, M. Uh, and F. Tamanoi. 1993. Identification of Ras farnesyltransferase inhibitors by microbial screening. *Proc. Natl. Acad. Sci. USA 90:2281.*
33. Varga, E. V., M. Rubenzik, V. Grife, M. Sugiyama, D. Stropova, W. R. Roeske, and H. I. Yamamura. 2002. Involvement of Raf-1 in chronic δ-opioid receptor agonist-mediated adenylyl cyclase superactivation. *Eur. J. Pharmacol. 451:101.*
34. Frost, J. A., H. Steen, P. Shapiro, T. Lewis, N. Ahn, P. E. Shaw, and M. H. Cobb. 1997. Cross-cascade activation of ERKs and ternary complex factors by Rho family proteins. *EMBO J. 16:6426.*
35. Lee, H. W., D. H. Ahn, S. C. Crawley, J. D. Li, J. R. Gum, Jr., C. B. Basbaum, N. Q. Fan, D. E. Szymkowski, S. Y. Han, B. H. Lee, et al. 2002. Phorbol 12-myristate 13-acetate up-regulates the transcription of MUC2 intestinal mucin via Ras, ERK, and NF-κB. *J. Biol. Chem. 277:32624.*
36. Christiansen, S. C., D. Proud, R. B. Sarnoff, U. Juergens, C. G. Cochrane, and B. L. Zuraw. 1992. Elevation of tissue kallikrein and kinin in the airways of asthmatic subjects after endobronchial allergen challenge. *Am. Rev. Respir. Dis. 145:900.*
37. Barnes, P. J. 1992. Bradykinin and asthma. *Thorax 47:979.*

38. Baumgarten, C. R., A. G. Togias, R. M. Naclerio, L. M. Lichtenstein, P. S. Norman, and D. Proud. 1985. Influx of kininogens into nasal secretions after antigen challenge of allergic individuals. *J. Clin. Invest. 76:191.*

39. Christiansen, S. C., D. Proud, and C. G. Cochrane. 1987. Detection of tissue kallikrein in the bronchoalveolar lavage fluid of asthmatic subjects. *J. Clin. Invest. 79:188.*

40. Petkova, D. K., L. Pang, S. P. Range, E. Holland, and A. J. Knox. 1999. Immunocytochemical localization of cyclo-oxygenase isoforms in cultured human airway structural cells. *Clin. Exp. Allergy 29:965.*

41. Inoue, H., C. Yokoyama, S. Hara, Y. Tone, and T. Tanabe. 1995. Transcriptional regulation of human prostaglandin-endoperoxide synthase-2 gene by lipopolysaccharide and phorbol ester in vascular endothelial cells: involvement of both nuclear factor for interleukin-6 expression site and cAMP response element. *J. Biol. Chem. 270:24965.*

42. Huang, W. C., J. J. Chen, H. Inoue, and C. C. Chen. 2003. Tyrosine phosphorylation of I-κB kinase αβ by protein kinase C-dependent c-Src activation is involved in TNF-α-induced cyclooxygenase-2 expression. *J. Immunol. 170:4767.*

43. Lin, C. H., S. Y. Sheu, H. M. Lee, Y. S. Ho, W. S. Lee, W. C. Ko, and J. R. Sheu. 2000. Involvement of protein kinase C-γ in IL-1β-induced cyclooxygenase-2 expression in human pulmonary epithelial cells. *Mol. Pharmacol. 57:36.*

44. Singer, C. A., K. T. Baker, A. McCaffrey, D. P. AuCoin, M. A. Dechert, and W. T. Gerthoffer. 2003. p38 MAPK and NF-κB mediate COX-2 expression in human airway myocytes. *Am. J. Physiol. 285:L1087.*

45. Saunders, M. A., L. Sansores-Garcia, D. W. Gilroy, and K. K. Wu. 2001. Selective suppression of CCAAT/enhancer-binding protein β binding and cyclooxygenase-2 promoter activity by sodium salicylate in quiescent human fibroblasts. *J. Biol. Chem. 276:18897.*

46. Bradbury, D. A., R. Newton, Y. M. Zhu, H. El-Haroun, L. Corbett, and A. J. Knox. 2003. Cyclooxygenase-2 induction by bradykinin in human pulmonary artery smooth muscle cells is mediated by the cyclic AMP response element through a novel autocrine loop involving endogenous prostaglandin E_2, E-prostanoid 2 (EP2), and EP4 receptors. *J. Biol. Chem. 278:49954.*

47. Li, J. D., W. Feng, M. Gallup, J. H. Kim, J. Gum, Y. Kim, and C. Basbaum. 1998. Activation of NF-κB via a Src-dependent Ras-MAPK-pp90rsk pathway is required for *Pseudomonas aeruginosa*-induced mucin overproduction in epithelial cells. *Proc. Natl. Acad. Sci. USA 95:5718.*

48. Arsura, M., F. Mercurio, A. L. Oliver, S. S. Thorgeirsson, and G. E. Sonenshein. 2000. Role of the IκB kinase complex in oncogenic Ras- and Raf-mediated transformation of rat liver epithelial cells. *Mol. Cell. Biol. 20:5381.*

49. Xie, W., and H. R. Herschman. 1996. Transcriptional regulation of prostaglandin synthase 2 gene expression by platelet-derived growth factor and serum. *J. Biol. Chem. 271:31742.*

50. Xie, W., B. S. Fletcher, R. D. Andersen, and H. R. Herschman. 1994. v-*src* induction of the TIS10/PGS2 prostaglandin synthase gene is mediated by an ATF/CRE transcription response element. *Mol. Cell. Biol. 14:6531.*

51. Sheng, H., J. Shao, and R. N. Dubois. 2001. K-Ras-mediated increase in cyclooxygenase 2 mRNA stability involves activation of the protein kinase B1. *Cancer Res. 61:2670.*

52. Madrid, L. V., C. Y. Wang, D. C. Guttridge, A. J. Schottelius, A. S. Baldwin, Jr., and M. W. Mayo. 2000. Akt suppresses apoptosis by stimulating the transactivation potential of the RelA/p65 subunit of NF-κB. *Mol. Cell. Biol. 20:1626.*

53. Lin, C. H., I. H. Kuan, C. H. Wang, H. M. Lee, W. S. Lee, J. R. Sheu, G. Hsiao, C. H. Wu, and H. P. Kuo. 2002. Lipoteichoic acid-induced cyclooxygenase-2 expression requires activations of p44/42 and p38 mitogen-activated protein kinase signal pathways. *Eur. J. Pharmacol. 450:1.*

54. Liao, J. K., and C. J. Homcy. 1993. The G proteins of the $G_{\alpha i}$ and $G_{\alpha q}$ family couple the bradykinin receptor to the release of endothelium-derived relaxing factor. *J. Clin. Invest. 92:2168.*

55. Liebmann, C., A. Graness, A. Boehmer, M. Kovalenko, A. Adomeit, T. Steinmetzer, B. Nurnberg, R. Wetzker, and F. D. Boehmer. 1996. Tyrosine phosphorylation of $G_{s\alpha}$ and inhibition of bradykinin-induced activation of the cyclic AMP pathway in A431 cells by epidermal growth factor receptor. *J. Biol. Chem. 271:31098.*

56. Wilk-Blaszczak, M. A., W. D. Singer, T. Quill, B. Miller, J. A. Frost, P. C. Sternweis, and F. Belardetti. 1997. The monomeric G-proteins Rac1 and/or Cdc42 are required for the inhibition of voltage-dependent calcium current by bradykinin. *J. Neurosci. 17:4094.*

57. Weissman, J. T., J. N. Ma, A. Essex, Y. Gao, and E. S. Burstein. 2004. G-protein-coupled receptor-mediated activation of rap GTPases: characterization of a novel $G_{\alpha i}$ regulated pathway. *Oncogene 23:241.*

58. Blaukat, A., A. Barac, M. J. Cross, S. Offermanns, and I. Dikic. 2000. G protein-coupled receptor-mediated mitogen-activated protein kinase activation through cooperation of $G_{\alpha q}$ and $G_{\alpha i}$ signals. *Mol. Cell. Biol. 20:6837.*

59. Hulsmann, A. R., H. R. Raatgeep, P. R. Saxena, K. F. Kerrebijn, and J. C. de Jongste. 1994. Bradykinin-induced contraction of human peripheral airways mediated by both bradykinin β_2 and thromboxane prostanoid receptors. *Am. J. Respir. Crit. Care Med. 150:1012.*

60. Molimard, M., C. A. Martin, E. Naline, A. Hirsch, and C. Advenier. 1994. Contractile effects of bradykinin on the isolated human small bronchus. *Am. J. Respir. Crit. Care Med. 149:123.*

THE JOURNAL OF BIOLOGICAL CHEMISTRY
Vol. 279, No. 40, Issue of October 1, pp. 42055–42061, 2004
Printed in U.S.A.

Identification and Characterization of Zipper-interacting Protein Kinase as the Unique Vascular Smooth Muscle Myosin Phosphatase-associated Kinase*

Received for publication, April 2, 2004, and in revised form, July 13, 2004
Published, JBC Papers in Press, July 30, 2004, DOI 10.1074/jbc.M403676200

Akira Endo‡, Howard K. Surks‡, Seibu Mochizuki§, Naoki Mochizuki¶, and Michael E. Mendelsohn‡‖

From the ‡Molecular Cardiology Research Institute, New England Medical Center and Department of Medicine, Tufts University School of Medicine, Boston, Massachussetts, the §Division of Cardiology, Department of Internal Medicine, Jikei University School of Medicine, Minato-ku, Tokyo 105-8461, Japan, and the ¶Department of Structural Analysis, National Cardiovascular Center Research Institute, Suita, Osaka 565-8565, Japan

Excitation-contraction coupling in smooth muscle involves activation of myosin light chain (MLC) phosphorylation, which increases activity of the myosin actin-activated ATPase, resulting in contraction. Phosphorylation of MLC phosphatase (SMPP-1M) by Rho-associated kinase or endogenous SMPP-1M-associated kinase inhibits SMPP-1M, enhancing MLC phosphorylation and contraction. However, the precise identity of SMPP-1M-associated kinase remains unclear. Biochemical evidence strongly supports the idea that SMPP-1M-associated kinase is related to the human serine/threonine leucine zipper-interacting protein kinase (hZIPK), which is important in cell apoptosis, and the SMPP-1M-associated kinase has therefore been called ZIP-like kinase (MacDonald, J. A., Borman, M. A., Murani, A., Somlyo, A. V., Hartshorne, D. J., and Haystead, T. A. J. (2001) *Proc. Natl. Acad. Sci. U. S. A.* 98, 2419–2424). Whether the vascular smooth muscle SMPP-1M-associated kinase is a truncated version of hZIPK, native hZIPK, or a unique homologue of hZIPK is unclear. Here we show that only native hZIPK mRNA and protein are detectable in human vascular smooth muscle cells (VSMCs). High stringency screening of a human aortic cDNA library for the SMPP-1M-associated kinase identified 18 positive clones, all of which proved to be clones of hZIPK. PCR-based studies of VSMC RNA revealed native hZIPK transcripts but no evidence for splice variants of hZIPK or a ZIP-like kinase. Northern blotting studies of multiple vascular and non-vascular tissue RNAs, including human bladder RNA, showed only 2.3 kb of mRNA predicted for full-length hZIPK. Immunoblotting showed native full-length 52-kDa hZIPK expression in VSMCs. Full-length and N-terminal hZIPK bound the C-terminal domain (amino acids 681–847) of the myosin binding subunit (MBS) of SMPP-1M. hZIPK immunoprecipitated with the MBS of SMPP-1M and dominant negative RhoA inhibited the hZIPK-MBS interaction. These data identify hZIPK as the unique SMPP-1-associated kinase expressed in human vesicular smooth muscle and support a role for Rho in promoting the hZIPK-MBS interaction.

Blood vessel tone regulates blood pressure and flow and is itself dynamically regulated by the contractile state of vascular smooth muscle cells (VSMCs)[1] in the blood vessel wall. Contraction and relaxation of VSMCs is determined by the phosphorylation state of myosin light chains (MLCs), a process that is tightly regulated by the opposing activities of myosin light chain kinase and myosin phosphatase (SMPP-1M) (1, 2). Myosin phosphatase is the critical enzyme that dephosphorylates MLC, leading to cell relaxation (3).

In recent years, accumulating evidence supports the view that myosin phosphatase activity is highly regulated. Nitrovasodilators, via cGMP and cGMP-dependent protein kinase Iα, lead to activation of PP1M and cell relaxation (4–8). Vasoconstrictors, conversely, increase MLC phosphorylation by at least two pathways, namely activation of MLCK (9, 10) and inhibition of SMPP-1M. Vasoconstrictors can inhibit SMPP-1M by activation of the potent PP1M inhibitor CPI-17 (11, 12) or via RhoA-mediated SMPP-1M phosphorylation (13). RhoA, when activated by vasoconstrictors, binds and activates its effector Rho-kinase, which leads to SMPP-1M phosphorylation (13). Although the mechanism by which RhoA and Rho-kinase are targeted to SMPP-1M on contractile fibers is unclear, both RhoA and SMPP-1M have been shown recently to interact with the actin-binding protein M-RIP (14).

Biochemical isolation of SMPP-1M has lead to the recovery of SMPP-1M-associated kinase activity (15–19). The SMPP-1M-associated kinase phosphorylates the myosin binding subunit (MBS) of SMPP-1M and inhibits SMPP-1M activity. As recent data support the physiologic importance of SMPP-1M regulation, attention has focused on identification of the SMPP-1M-associated kinase(s).

Recently, MacDonald *et al.* identified a SMPP-1M-associated kinase and named it ZIP-like kinase. ZIP-like kinase was isolated from bladder smooth muscle as a 32-Da phosphoprotein that co-purified with SMPP-1M, phosphorylated SMPP-1M at inhibitory residues, and was activated by the smooth muscle contractile agonist carbachol (16). Furthermore, introduction of ZIP-like kinase into rabbit ileal smooth muscle led to calcium-independent contractions (20).

Despite data supporting a physiological role for a ZIP-like kinase in smooth muscle, the precise identity of this kinase and

* This work was supported in part by National Institutes of Health Grant ML55309 (to M. E. M.) and a fellowship grant from the Uehara Memorial Foundation (to A. E.). The costs of publication of this article were defrayed in part by the payment of page charges. This article must therefore be hereby marked "*advertisement*" in accordance with 18 U.S.C. Section 1734 solely to indicate this fact.

‖ To whom correspondence should be addressed. E-mail: mmendelsohn@tufts-nemc.org.

[1] The abbreviations used are: VSMC, vascular smooth muscle cell; aa, amino acid(s); GST, glutathione *S*-transferase; HEK293, human embryonic kidney 293 (cell); MBS, myosin-binding subunit; MLC, myosin light chain; SMPP-1M, MLC phosphatase; MOPS, 4-morpholinepropanesulfonic acid; ZIPK, zipper-interacting protein kinase; hZIPK, human ZIPK.

its presence and function in VSMCs remains unclear. Sequencing of ZIP-like kinase-derived peptides revealed high homology to the 52-kDa zipper-interacting protein kinase (hZIPK), raising the possibility that ZIP-like kinase could be a splice variant of hZIPK, a separate kinase with high homology to hZIPK, or a degradation product of hZIPK (16). hZIPK was identified originally as a protein involved in programmed cell death that interacts with the transcription factor ATF4 and mediates apoptosis when overexpressed (21). hZIPK has also been shown to have a potential role in regulating VSMC contraction. hZIPK was found to phosphorylate MLC at both Ser^{19} and Thr^{18} in a calcium-independent manner, leading to cell contraction (22).

The following study was initiated to determine the precise identity of the PP1M-associated kinase(s) in VSMCs. Through a combination of mRNA and protein analysis, we have found evidence to strongly support the proposition that "ZIP-like kinase" in VSMCs is actually derived from hZIPK, which is present in VSMCs and interacts with SMPP-1M in a RhoA-regulated manner.

MATERIALS AND METHODS

Antibodies—Sources of antibodies were as follows. The rabbit polyclonal anti-ZIP kinase (amino acids 279–298) was from Calbiochem, the anti-FLAG-M2 antibody was from Sigma, the anti-myosin phosphatase polyclonal antibody came from Covance (Berkeley, CA), and normal mouse IgG and normal rabbit IgG were from Santa Cruz Biotechnology Inc., Santa Cruz, CA.

Cell Culture and Transfection—Human embryonic kidney 293 (HEK293) cells were purchased from the American Type Culture Collection (Manassas, VA). Immortalized aorta smooth muscle cells, coronary smooth muscle cells, pulmonary artery smooth muscle cells, and radial artery smooth muscle cells were developed in our laboratory from human tissues by the explant method. These cells were cultured in Dulbecco's modified Eagle's medium supplemented with 10% fetal calf serum. HEK293 cells were transfected by the calcium phosphate method.

Plasmids—To generate plasmids expressing hZIPK, cDNA-fragments were amplified by a polymerase chain reaction from pACT2 (Clontech) containing hZIPK fragments and cloned into pT7Blue-3 (Novagen, Madison, WI). pT7Blue3-hZIPK was digested with EcoRI and BamHI, and the fragments were cloned into the pFLAG-CMV4 vector (Sigma). GST fusion proteins of full-length and C-terminal hZIPK were generated as follows. DNA fragments corresponding to full-length and C-terminal hZIPK were amplified by PCR using the primer pairs of 5′-GGGAATTCTATGTCCACGTTCAGGCAGGAG-3′ (5′) and 5′-GGGTCGACCTAGCGCAGCCCGCACTCCACG-3′ (3′) for the former and 5′-GGGAATTCAGCGGCCGCAAGCCCGAGCGGC-3′ (5′) and 5′-GGGTCGACCTAGCGCAGCCCGCACTCCACG-3′ (3′) for the latter. The PCR products were cloned into pT7Blue-3 and digested with EcoRI and SalI. These fragments were cloned into pGEX4T-3 and pGEX4T-1 vectors (Amersham Biosciences). To generate the plasmid expressing the GST-N-terminal region of hZIPK, NotI-digested pGEX4T-3 hZIPK was treated with a Klenow fragment (New England Biolabs, Beverly, MA) to blunt the ends, followed by self-ligation. pEF-BOS-mouse ZIPK was a gift from S. Akira, Department of Biochemistry, Hyogo College of Medicine. $pCXN_2$-IRES-EGFP (23) expression vectors were derived from pCAGGS and contain the internal ribosomal entry site (IRES) and the coding region of the enhanced green fluorescent protein (EGFP) at the 3′-end of the multiple cloning site. The cDNA fragments encoding the small GTPase RhoA, RhoN19 (dominant negative form), and RhoQ63L (constitutively active form) were amplified by polymerase chain reaction and subcloned into $pCXN_2$-IRES-EGFP.

Human Aorta cDNA Library Screening—A human aorta cDNA library containing 3.5×10^6 independent clones (Clontech) was screened by the colony hybridization technique (24). ^{32}P-labeled EcoRI-NotI fragments of hZIPK cDNA were made from the cDNA clone AI660136 (Genome System) encoding the N terminus of hZIPK and used as a probe. The library was transferred to Hybond N synthetic nylon membranes (Amersham Biosciences) and then pre-hybridized and hybridized in 5× Denhardt's solution, 5× SSC, 0.1 M sodium phosphate, 0.5% SDS, and 100 μg/ml denatured salmon sperm DNA under high (hybridization temperature 65 °C) and low (hybridization temperature 58 °C) stringency conditions.

Polymerase Chain Reaction—PCR was performed in a final volume of 50 μl of reaction mix containing 0.2 mM each dNTP, 1.5 mM $MgCl_2$, PCR buffer without magnesium, 0.25 μM each primer for the investigation of ZIPK splice variants, 500 μM each primer for degenerate PCR, and 2 units of *Taq* DNA polymerase (Invitrogen). Reaction mixtures were heated for 5 min at 95 °C, followed by 30 cycles of amplification. Each cycle consisted of denaturation at 95 °C for 30 s, annealing between 38 and 57 °C, and extension at 70 °C between 1 and 3 min. After the last cycle, samples were incubated for an additional 10 min at 70 °C. The following primers were designed for the investigation of hZIPK splice variants: primer 1, 5′-AGGCGCGTCGCGGCGGCAGGGCG-3′ (3′) and 5′-CTTCAGGTCAAAGTGTGCGATGCG-3′ (5′); primer 2, 5′-AGGCGCGTCGCGGCGGCAGGGGCG-3′ (3′) and 5′-GGATATAGGTGATGACACCGA-3′ (5′); primer 3, 5′-AGGCGCGTCGCGGCGGCAGGGGCG-3′ (3′) and 5′-GCTCGGGCTTGCGGCCGCTG-3′ (5′); primer 4, 5′-ATGTCCACGTTCAGGCAGGAGG-3′ (3′) and 5′-CTTCAGGTCAAAGTGTGCGATGCG-3′ (5′); primer 5, 5′-ATGTCCACGTTCAGGCAGGAGG-3′ (3′) and 5′-GGATATAGGTGATGACACCGA-3′ (5′); primer 6, 5′-ATGTCCACGTTCAGGCAGGAGG-3′ (3′) and 5′-GCTCGGGCTTGCGGCCGCTG-3′ (5′); primer 7, 5′-AGGAACTGAGAGCCTGCC-3′ (3′) and 5′-CTTCAGGTCAAAGTGTGCGATGCG-3′ (5′); primer 8, 5′-AGGAACTGAGAGCCTGCC-3′ (3′) and 5′-GGATATAGGTGATGATGACACCGA-3′ (5′); primer 9, 5′-AGGAACTGAGAGCCTGCC-3′ (3′) and 5′-CTTCAGGTCAAAGTGTGCGATGCG-3′ (5′); primer 10, 5′-ATGCTGCTGGACAAGAAC-3′ (3′) and 5′-GGATATAGGTGATGACACCGA-3′ (5′); and primer 11, 5′-ATGCTGCTGGACAAGAAC-3′ (3′) and 5′-CTTCAGGTCAAAGTGTGCGATGCG-3′ (5′) (Fig. 3). Exons were predicted using the NCBI LocusLink program.

The following primers were used for degenerate PCR: primer IA, 5′-ATGGGNGARGARYTNGG-3′ (5′) and 5′-YTGDATNGGNC-3′ (3′); primer IB, 5′-ATGGGNGARGARYTNGG-3′ (5′) and 5′-RAADATNNNYTTRTC-3′ (3′); primer IIA, 5′-GAYAARNNNATHTT-3′ (5′) and 5′-ARRTTYTGNGCDAT-3′ (3′); primer IIB, 5′-MGNCCNATHCA-3′ (5′) and 5′-ARRTTYTGNGCDAT-3′ (3′); primer III, 5′-ATGGGNGARGARYTNGG-3′ (5′) and 5′-ARRTTYTGNGCDAT-3′ (3′) (Fig. 2). The primers 5′-ATGGGNGARGARYTNGG-3′, 5′-GAYAARNNNATHTT-3′, 5′-MGNCCNATHCA-3′, 5′-YTGDATNGGNC-3′, 5′-RAADATNNNYTTRTC-3′, and 5′-ARRTTYTGNGCDAT-3′ corresponded to amino acid sequences MGEEL, DKXIF, RPIQ, QIPR, FIXKD, and LNQAI, respectively. The human aorta cDNA library was used as the template for PCR with IA, IIA, and III. PCR products from IA and IIA were used as the template for PCR with IB and IIB, respectively.

RNA Expression Analysis by Northern Blotting—Total RNA from a series of mouse tissues and poly(A)$^-$ RNA from cultured cells and human bladder was electrophoresed in an agarose gel containing 2% formaldehyde and 20 mM MOPS and blotted onto Hybond N synthetic nylon membrane (Amersham Biosciences). A multiple tissue Northern blot that has poly(A)$^+$ RNA from a series of human tissues was purchased from Clontech. The membranes were pre-hybridized and hybridized in ExpressHyb hybridization solution (Clontech) with [^{32}P]dCTP-labeled probe. The cDNA probes used in this study are described as follows. A 0.9-kb EcoRI-NotI fragment encoding the 5′-end of the human ZIPK cDNA and a 1.4-kb EcoRI-BamHI fragment encoding full-length human ZIPK were made from pFLAG-CMV4-ZIPK. A 1-kb SalI-NotI fragment encoding the 5′-end of mouse ZIPK and a 1.3-kb SalI-SalI fragment encoding full-length mouse ZIPK were made from pEF-BOS-ZIPK.

Preparation of GST Fusion Proteins for Binding Studies—BL21 cells were transformed with GST-ZIPK plasmids, described above, and GST-MBS plasmids expressing the C-terminal 183 aa of MBS or the C-terminal 183 aa in which the four leucine residues of the leucine zipper domain have been mutated to alanines (L1007A, L1014A, L1021A, and L1028A) were made as described previously (14). The transformed cells were grown in Luria-Bertani media at 30 °C until the absorbance at 600 nm reached 0.6–0.8. Protein expression was induced by the addition of 0.1 mM isopropyl-β-D-thiogalactopyranoside for 3 h, and GST fusion proteins were isolated by using glutathione-Sepharose 4B beads.

Immunoprecipitation, Immunoblotting, and Cell Staining—Cells were washed with ice-cold Tris-buffered saline (25 mM Tris-HCl, pH7.5, and 150 mM NaCl), and lysed in lysis buffer (20 mM Tris-HCl, pH7.5, 137 mM NaCl, 1% Triton X-100, 2 mM EDTA, 10% glycerol, 25 mM β-glycerophosphate, protease inhibitor mixture set III (Calbiochem), and protease inhibitor mixture tablets (Roche Applied Science). Lysates were cleared by centrifugation at $15,000 \times g$ for 10 min. Aliquots of total cell lysate were subjected to immunoblotting with antibodies as indicated in Figs. 1 and 5–7. The remaining cell lysate was subjected to either immunoprecipitation using antibodies as indicated in Figs. 6 and 7 and protein A- and G-Sepharose (Amersham Biosciences) or GST fusion protein interaction studies by incubation with the indicated GST fusion protein. This treatment was followed by SDS-PAGE and transfer

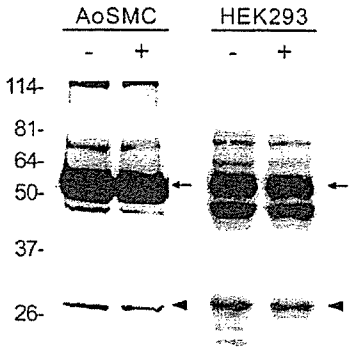

FIG. 1. **Expression of the ZIPK protein in HEK293 cells and human vascular smooth muscle cells.** HEK293 cell lysates from cells transfected with ZIPK cDNA and native human aortic smooth muscle cell lysates (*AoSMC*) (10μ g) were separated by SDS-PAGE with (+) and without (−) protease inhibitors present and immunoblotted with the polyclonal anti-ZIPK antibody. *Arrow* and *arrowhead* indicate ZIPK at the 52- and a 32-kDa band recognized by the antibody, respectively. The ZIP-like kinase co-purified with SMPP-1M from bladder smooth muscle was a 32-kDa protein (16).

to polyvinylidene difluoride membranes. The blocked membranes were incubated with the primary antibody at 4 °C overnight and then probed with the secondary antibody linked to peroxidase. Immunoreactive bands were visualized by a chemiluminescence system (Amersham Biosciences) and subjected to densitometric quantitation. For immunofluorescence labeling, cells were washed with phosphate-buffered saline, fixed by 4% paraformaldehyde at room temperature, and then permeabilized with 0.1% Triton X-100. Permeabilized cells were incubated with an anti-FLAG antibody followed by Alexa 488 goat anti-mouse IgG (Molecular Probes, Eugene, OR).

Statistical Analysis—Data are presented as means ± S.E. Statistical difference was evaluated by Student's *t* test. A p value of < 0.01 was regarded as significant.

RESULTS

Immunoblotting Studies—A 32-kDa SMPP-1M-associated kinase was detected previously by immunoblotting of rabbit bladder lysates with the anti-hZIPK antibody (16). We have used this antibody in immunoblotting studies of proteins expressed by native vascular smooth muscle cells and in studies of HEK293 cells expressing the cDNA for hZIPK (Fig. 1). In both VSMC cells and in heterologous expression studies of HEK293 cells the most prominent protein band detected by the anti-ZIPK antibody was 52 kDa (Fig. 1, *upper arrows*). A 32-kDa band was also detected in both cell types (*arrowhead*) but was less prominent, especially in human VSMC lysates. The inclusion of protease inhibitors did not alter the amount of 32-kDa protein detected (+ *lanes*, Fig. 1). In the HEK293 cells expressing hZIPK, another protein of ~48 kDa was also prominent. Detection of this 48-kDa protein was also not affected by the inclusion of a mixture of protease inhibitors.

cDNA Library Screening for ZIPK and ZIP-like Kinase—A human aorta cDNA library containing 3.5×10^6 independent clones was screened for the presence of ZIPK and ZIP-like kinase by the colony hybridization technique. A 981-bp fragment of the 5′-end of hZIPK was used as the probe. This region of hZIPK cDNA was chosen for the probe design based on a previous report of homology between peptide fragments of ZIP-like kinase and the amino-terminal kinase domain of ZIPK (16) (Fig. 2*A*). The human aorta cDNA library was screened under both high and low stringency conditions. Using high stringency conditions, we obtained 18 positive clones. These positive clones were fully sequenced, and all 18 positive clones were identified as either full-length or fragments of hZIPK. Under low stringency conditions, 41 positive clones were obtained, and 31 were identified as full-length or fragments of hZIPK. We also cloned myosin light chain kinase (eight clones), the kinase domain of which has 48% amino acid sequence identity and 59% nucleotide sequence identity (25), as well as part of the ZIPK gene on chromosome 19 (two clones). ZIP-like kinase was not identified by either of the library screens.

PCR Studies to Search for ZIP-like Kinase and Detect Potential ZIPK Splice Variants—We designed degenerate PCR primers corresponding to the three peptide sequences derived originally from ZIP-like kinase with minor or uncertain sequence differences from hZIPK (Fig. 2*B*) (16). All DNA fragments amplified from the human aorta library using these degenerate primers were sequenced (Fig. 2*C*) but proved to be nonspecific, and no sequences corresponded to those of hZIPK or ZIP-like kinase.

To determine whether ZIP-like kinase is a splice variant of hZIPK, we searched for hZIPK splice variants in the human aorta cDNA library. hZIPK mRNA is derived from eight exons on chromosome 19. We designed PCR primers corresponding to each exon and two putative exons designated potential exons A and B, one 5′ to exon1 (potential exon A) and the other between exon 2 and exon 3 (potential exon B) (Fig. 3*A*) based on predicted potential splice sites and variants (the NCBI LocusLink program). PCR was performed with 11 primer pairs designed to amplify both the known exons and potential exons A and B. Only the hZIPK exons were amplified. A number of DNA fragments were sequenced and proved to be of 100% identity to hZIPK (Fig. 3*B*). These results make the existence of a potential splice variant in human aorta of hZIPK unlikely.

Northern Blotting Studies—We investigated the expression of mRNA encoding ZIP-like kinase in various human tissues and cultured cells by performing Northern blot analyses. In all of these human tissues and cultured cells, a 5′-probe, based on hZIPK, was used at moderate stringency to detect hZIPK and any related transcripts. In all tissues and cells examined, a 2.3-kb band consistent with the predicted size of the hZIPK transcript was present, but no evidence of any other transcripts was noted (Fig. 4, *A* and *B*). ZIP-like kinase was co-purified with SMPP-1M originally from bladder smooth muscle (16). We therefore obtained human bladder tissue, isolated the mRNA, and performed separate Northern blot experiments (Fig. 4*B*, *right panel*). In human bladder, only a 2.3-kb band consistent with the predicted size of the hZIPK transcript was detected, and no evidence of any other transcript was noted. Re-probing of these blots with full-length hZIPK probe led to detection of the same bands and no others, indicating that these 2.3-kb bands are hZIPK mRNA (data not shown). We also investigated hZIPK and ZIP-like kinase expression in various mouse tissues, including brain, aorta, heart, lung, liver, spleen, kidney, uterus, and bladder. Among the mouse tissues, an ~2.3-kb band was detected. No other smaller mRNA species were detected (data not shown). We therefore could find no evidence that suggested the existence of an mRNA for a ZIP-like kinase in human and mouse tissues or in cultured cells.

Interaction of hZIPK with MBS—We investigated whether full-length hZIPK interacts with MBS. FLAG-tagged hZIPK was well expressed in HEK293 cells and distributed uniformly throughout the cytoplasm in these cells (Fig. 5, *A* and *B*). FLAG-hZIPK bound the C-terminal half of human MBS (GST-MBS with aa 681–1030). In contrast, neither GST-MBS with aa 847–1030 nor a mutant GST-MBS with aa 847–1030 in which the leucine zipper of MBS is disrupted by alanine substitution (designated GST-MBS 847–1030 LZM in Fig. 5) bound hZIPK. These data confirm an *in vitro* interaction between full-length hZIPK and the coiled coil-containing domain of MBS (aa 681–847 of human MBS) (Fig. 5*C*). The binding of native ZIPK from human vascular smooth muscle cells to these GST-MBS fusion proteins was similarly observed (Fig. 5*E*). In reciprocal studies,

A

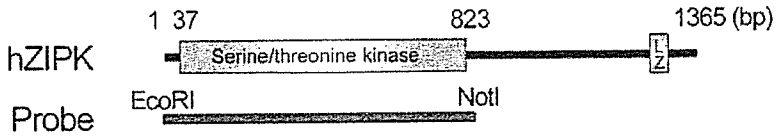

B

stringency	hybridization temperature	number of screened clones	% of library screened	positive clones (number isolated)
High	65°C	3.0×10^6	87%	hZIPK (18)
Low	58°C	3.2×10^6	91%	hZIPK (31) MLCK (8) Human chromosome 19 (2)

C

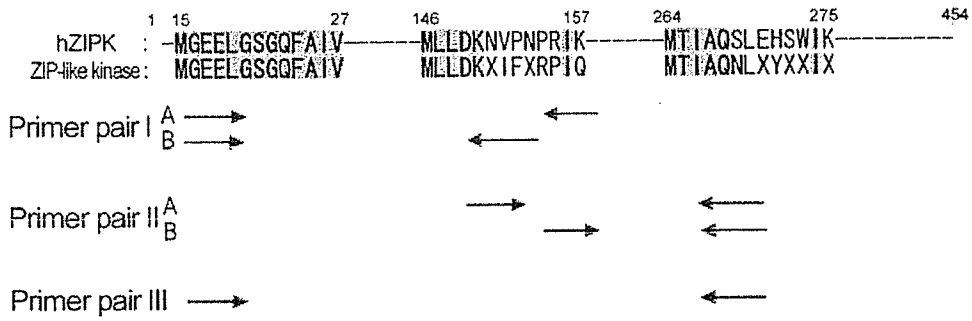

D

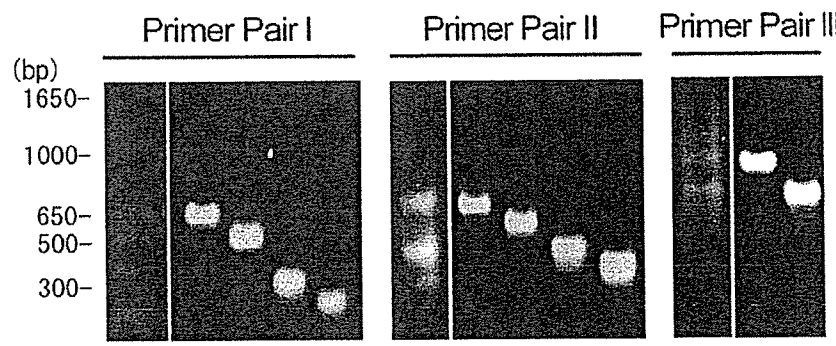

FIG. 2. **Cloning of human ZIPK and related kinases from the human aortic vascular cDNA library.** *A*, diagram of EcoRI-NotI fragments encoding the N-terminal kinase domain of ZIPK used as the probe to screen the human aortic cDNA library at both low and high stringency. Probe design was based on the previous report of homology between peptide fragments of ZIP-like kinase and the amino-terminal kinase domain of ZIPK (16). *B*, summary of clones isolated from the cDNA library screen with both low and high stringency hybridization conditions. *C*, degenerate PCR Studies to detect ZIP Kinase and ZIP-like kinase. Amino acid sequences of peptides derived from the putative ZIP-like kinase (16) and aligned with the amino acid sequence of hZIPK (GenBank™ accession number AB022341) are shown. Degenerate PCR primers corresponding to these amino acid sequences were designed (*arrows*) and used in PCR reactions with the human aorta library DNA as the template. The PCR products of primer pair IA and IIA shown were used as templates for PCR reactions with primer pair IB and IIB, respectively. *D*. PCR products of primer pair IB and IIB, as well as primer pair III, were size-fractionated by agarose gel electrophoresis (shown in the *far left lanes* in *each panel*). Four fragments from primer pair I and II and two fragments from primer pair III were gel-extracted and reamplified and are shown in the *right section* of the gel for each primer pair. The reamplified fragments were used for DNA sequencing. All cDNA recovered proved to be nonspecific, and no sequences corresponded to hZIPK or ZIP-like kinase were detected.

full-length ZIPK and N-terminal ZIPK both bound MBS, whereas GST-C-terminal ZIPK did not, supporting the idea that the amino-terminal half of ZIPK binds to MBS (Fig. 5*D*). Next, MBS and hZIPK were each immunoprecipitated from cells to test for an interaction between the two proteins *in vivo*. When MBS was immunoprecipitated from HEK293 cells, FLAG-hZIPK was present in the immunopellet (Fig. 6*A*), and, reciprocally, the immunoprecipitation of FLAG-hZIPK led to the recovery of MBS in the immunopellet (Fig. 6*B*). These data indicate that hZIPK and MBS are complexed in the cell. Finally, we studied whether the small GTPase RhoA might regulate the interaction we observed between hZIPK and MBS. In GST pull-down assay studies, no differences were detected in the level of ZIP kinase bound by MBS from native Rho with

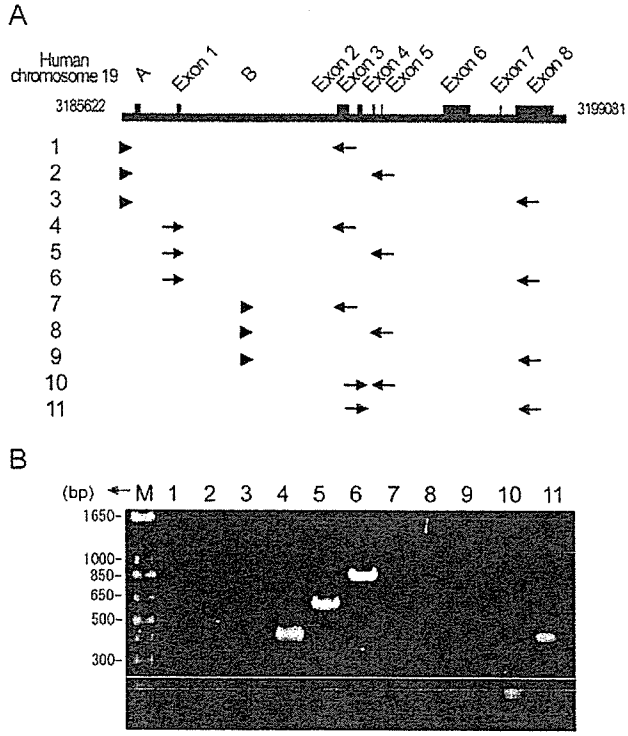

FIG. 3. **Investigation of potential mRNA splice variants of human ZIP kinase.** *A*, structure of the hZIPK gene on chromosome 19. The two predicted exons are labeled A and B. Exons 1, 2, 3, 4, 5, 6, 7, and 8 each encode 1–62, 63–423, 424–553, 554–603, 604–629, 630–783, 784–829, and 830–1365 bp of ZIP kinase, respectively. Each PCR primer was designed to correspond to each exon and predicted exon using the NCBI LocusLink program. *Arrows* indicate the forward and reverse primers corresponding to known exons; *arrowheads* indicate the forward primer corresponding to predicted potential exons A and B. *B*, PCR products were size-fractionated by agarose gel electrophoresis. A large number of DNA fragments amplified with this approach were sequenced; all sequences proved to be identical to hZIPK. *M*, 1-kb DNA ladder marker.

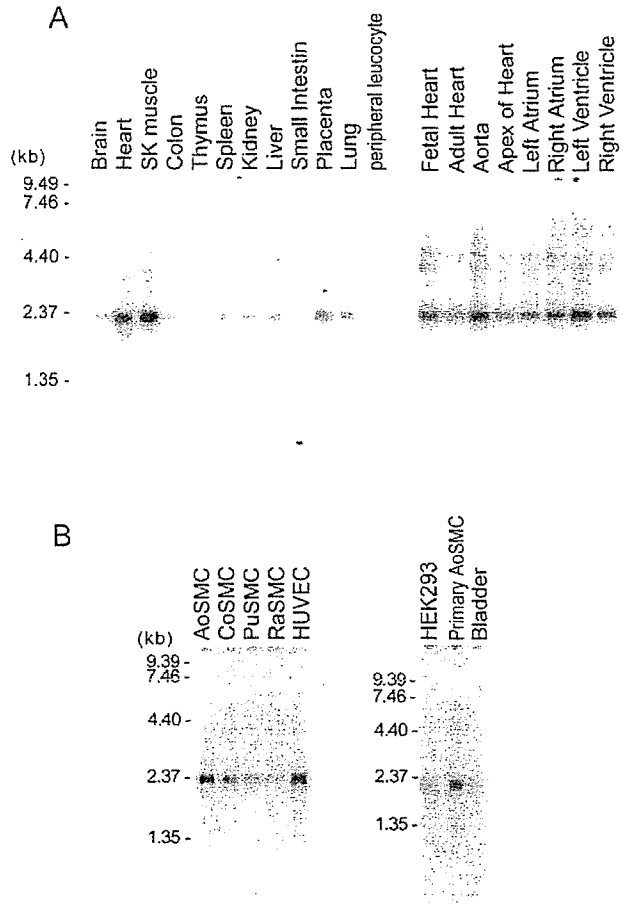

FIG. 4. **Northern blotting studies of hZIPK mRNA expression in non-vascular and vascular tissues.** *A*, multi-tissue Northern filters (Clontech). These filters, along with 1.5 μ g of poly(A)$^+$ RNA from various human tissues, were hybridized with the radiolabeled 5′-end of hZIPK and exposed to a PhosphorImager (Amersham Biosciences). *B*, Northern filters prepared from human primary vascular cell lines and human bladder tissue RNA. Poly(A)$^+$ RNAs (2μ g) from various cultured cells and human bladder were loaded in each lane. The filters were hybridized with the radiolabeled 5′-end of hZIPK as a probe and exposed to a PhosphorImager. *AoSMC*, primary human aortic smooth muscle cell; *CoSMC*, human coronary arterial smooth muscle cell; *PuSMC*, human pulmonary arterial smooth muscle cell; *RaSMC*, human radial artery smooth muscle cell; *HUVEC*, human umbilical vein endothelial cells.

either RhoN19 (dominant negative) or RhoQL (constitutively active) (data not shown). MLC phosphorylation by ZIP kinase also was assayed by isolating ZIP kinase from cells expressing wild type Rho, RhoN19, or RhoQL, but differences in the level of MLC phosphorylation were not detected in this assay (data not shown). When hZIPK was immunoprecipitated, however, co-immunoprecipitation of MBS was significantly diminished in the presence of a dominant negative mutant of RhoA, RhoN19 (Fig. 7). The constitutively active Rho protein, RhoQL, did not increase the level of ZIPK bound to MBS above the level seen with native (wild type) Rho in these studies (Fig. 7). These immunoprecipitation data support the belief that active Rho promotes the hZIPK-MBS interaction characterized in these studies.

DISCUSSION

Because the regulatory pathways that modulate SMPP-1M activity remain incompletely understood, we undertook this study to identity the endogenous SMPP-1M-associated kinase(s). A 32-kDa ZIP-like kinase had been found previously to co-purify with and inhibit SMPP-1M activity, whereas 52-kDa hZIPK had been shown to phosphorylate MLC and cause cell contraction (16, 22, 25). We set out to clone the SMPP-1M-associated ZIP-like kinase from vascular tissue, employing two methods to screen a highly representative human aorta cDNA library for evidence of ZIP-like kinase. In the first approach, we performed colony hybridization using a probe against the 5′-half of hZIPK, which, because of high homology, would be expected to identify both ZIP-like kinase and hZIPK. We also used a reverse transcription PCR approach with this human aorta library as the template and both degenerate primers and primers designed to identify hZIPK splice variants. In our studies, only hZIPK but not any ZIP-like kinase was present in this library.

As alternative approaches, we also used both the 5′-catalytic domain and full-length hZIPK as probes in both vascular and non-vascular cellular RNA Northern hybridization experiments. A variety of human tissues as well as human blood vessel, heart, and VSMCs from a variety of human blood vessel types were studied. Importantly, human bladder tissue was also studied because the ZIP-like kinase was originally purified from bladder smooth muscle tissue (16). In all of these tissues and cells only a single transcript of the expected 2.4 kb for hZIPK was detectable, supporting further the proposal that hZIPK is the sole SMPP-1 M-associated kinase expressed in human tissues.

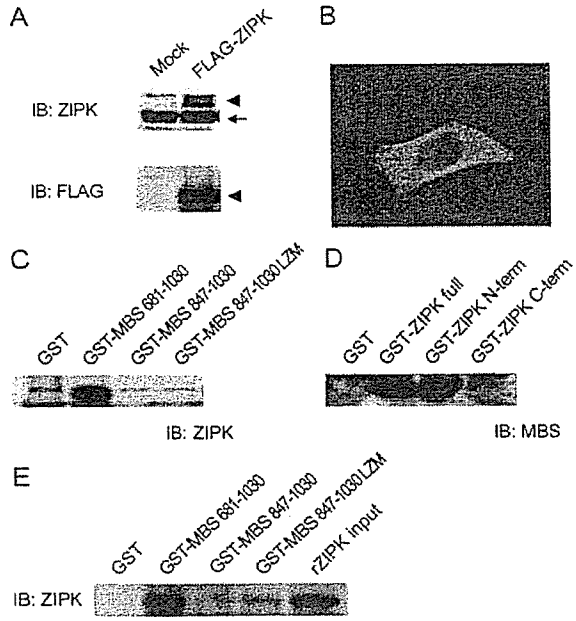

FIG. 5. **Interaction of ZIPK with MBS *in vitro*.** *A*, HEK293 cells were transfected with hZIPK plasmid or control plasmid, and cell lysates were immunoblotted (*IB*) with either anti-ZIPK (*top*) or anti-FLAG (*bottom*) antibodies. The *arrow* and *arrowheads* indicate endogenous hZIPK and FLAG-tagged hZIPK, respectively. *B*, HEK293 cells transiently transfected with hZIPK were fixed and stained with anti-FLAG antibody and visualized with immunofluorescence microscopy. Note that ZIP kinase is distributed uniformly throughout the cytoplasm in these cells. *C*, HEK293 cells transfected with hZIPK were lysed, and the lysates were then used in GST pull-down protein-protein interaction studies. Binding of ZIPK was probed using anti-FLAG antibody. The *lane* marked *GST* represents GST alone. GST-MBS constructs expressing either aa 681–1030 or aa 847–1030 are represented by the *lanes* marked *GST-MBS 681–1030* or *GST-MBS 847–1030*. The *lane* marked *GST-MBS 847–1030 LZM* represents the construct expressing the domain of MBS with the leucine residues in the leucine zipper of the domain mutated to alanines. *D*, HEK293 cells transfected with hZIPK were lysed, and the lysates were then used in GST-pull-down protein-protein interaction studies. *GST*, GST alone; *GST-ZIPK Full*, full-length ZIP kinase; *GST-ZIPK N-term*, N-terminal ZIP kinase with aa 1–288; GST-ZIPK C-term, C-terminal ZIP kinase with aa 288–454. *E*, human aortic vascular smooth muscle cells were lysed, and the lysates were then used in GST pull-down protein-protein interaction studies. Binding of ZIPK was probed using the anti-ZIPK antibody. The *lane* marked *GST* represents GST alone. GST-MBS constructs expressing either aa 681–1030 or aa 847–1030 are represented by the *lanes* marked *GST-MBS 681–1030* or *GST-MBS 847–1030*. The *lane* marked *GST-MBS 847–1030 LZM* represents the construct expressing the domain of MBS with the leucine residues in the leucine zipper of the domain mutated to alanines (14). The *far right lane* shows a recombinant ZIPK (*rZIPK*) positive control.

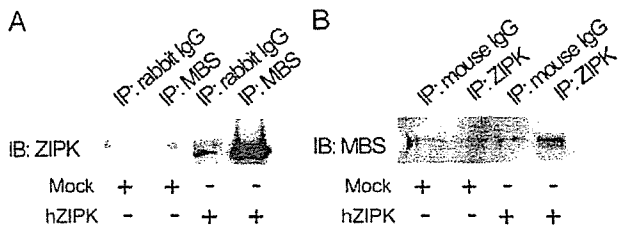

FIG. 6. **Interaction of ZIPK with MBS in cells.** HEK293 cells transfected with hZIPK were lysed, and lysates were then used in immunoprecipitation (*IP*) studies of human MBS (*panel A*) or ZIPK (*panel B*), followed by immunoblotting (*IB*) of ZIPK or MBS, respectively.

We also tested for the binding of hZIPK to MBS in several ways. Heterologous expression of hZIPK demonstrated that hZIPK binds directly to the coiled coil-containing domain of

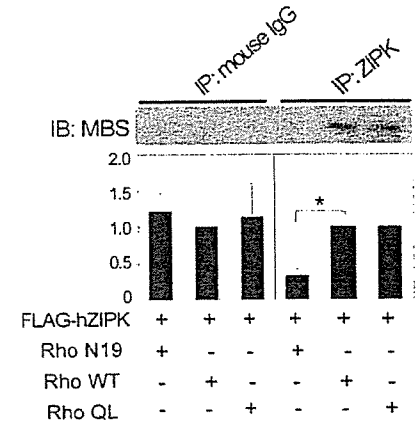

FIG. 7. **Effect of small GTPase RhoA on the interaction between human ZIPK and MBS.** HEK293 cells were cotransfected with hZIPK and wild type (*WT*) RhoA or either dominant negative (*N19*) or constitutively active (*QL*) RhoA. Immunoprecipitation (*IP*) with normal mouse IgG (control; *left*) or anti-FLAG antibody for ZIP kinase (*right*) was followed by immunoblotting (*IB*) with anti-MBS antibody and densitometric quantitation. The signal intensity of Rho wild type (*Rho WT*) was arbitrarily designated as unity. *, $p < 0.01 (n = 3$ to 5).

MBS in GST pull-down protein-protein interaction studies and to complexes with MBS in co-immunoprecipitation experiments, strongly supporting the idea that hZIPK interacts with MBS in the cell. Furthermore, disruption of RhoA activation by overexpression of a dominant negative RhoA mutant inhibited this hZIPK-MBS interaction in cells. We did not detect an effect of RhoN19 on hZIPK-MBS binding using GST fusion proteins or in a MLC phosphorylation assay using immunoprecipitated hZIPK derived from cells expressing wild type or mutant Rho protein. These negative data support either the reduced sensitivity of these assays compared with co-immunoprecipitation or the need for additional cellular proteins for Rho to regulate the hZIPK-MBS interaction. Taken together, the data support the hypothesis that the interaction between hZIPK and MBS may be regulated by RhoA and that hZIPK may play a role in PP1M regulation by RhoA.

Studies in both animals and humans have shown that SMPP-1M activity is regulated in health and in disease. Hyperactivity of the RhoA pathway leading to SMPP-1M inhibition and blood vessel contraction has been shown in hypertensive states, and enzyme inhibitors that prevent SMPP-1M inhibition are promising new treatments for cardiovascular disorders (26, 27). Our data establish that hZIPK is the SMPP-1M-associated kinase and support the hypothesis that the hZIPK-SMPP-1M interaction is regulated by RhoA. Future studies will be directed at defining the role of hZIPK in the modulation of SMPP-1M activity by vasoconstrictor agonists and other potential mechanisms through which hZIPK regulates vascular smooth muscle cell function.

REFERENCES

1. Hartshorne, D. J. (1987) in *Physiology of the Gastrointestinal Tract* (Johnson, D. R., ed) pp. 423–482, Raven Press, Ltd., New York
2. Somlyo, A. P., and Somlyo, A. V. (1994) *Nature* **372**, 231–236
3. Alessi, D., MacDougall, L. K., Sola, M. M., Ikebe, M., and Cohen, P. (1992) *Eur. J. Biochem.* **210**, 1023–1035
4. Surks, H. K., Mochizuki, N., Kasai, Y., Georgescu, S. P., Tang, K. M., Ito, M., Lincoln, T. M., and Mendelsohn, M. E. (1999) *Science* **286**, 1583–1587
5. Khatri, J. J., Joyce, K. M., Brozovich, F. V., and Fisher, S. A. (2001) *J. Biol. Chem.* **276**, 37250–37257
6. Etter, E. F., Eto, M., Wardle, R. L., Brautigan, D. L., and Murphy, R. A. (2001) *J. Biol. Chem.* **276**, 34681–34685
7. Lee, M. R., Li, L., and Kitazawa, T. (1997) *J. Biol. Chem.* **272**, 5063–5068
8. Wu, X., Somlyo, A. V., and Somlyo, A. P. (1996) *Biochem. Biophys. Res. Com.* **220**, 658–663
9. Kamm, K. E., and Stull, J. T. (1985) *Annu. Rev. Pharmacol. Toxicol.* **25**, 593–620
10. Taylor, D. A., and Stull, J. T. (1988) *J. Biol. Chem.* **263**, 14456–14462

11. Eto, M., Senba, S., Morita, F., and Yazawa, M. (1997) *FEBS Lett.* **410,** 356–360
12. Eto, M., Kitazawa, T., Yazawa, M., Mukai, H., Ono, Y., and Brautigan, D. L. (2001) *J. Biol. Chem.* **276,** 29072–29078
13. Kimura, K., Ito, M., Amano, M., Chihara, K., Fukata, Y., Nakafuku, M., Yamamori, B., Feng, J., Nakano, T., Okawa, K., Iwamatsu, A., and Kaibuchi, K. (1996) *Science* **273,** 245–248
14. Surks, H. K., Richards, C. T., and Mendelsohn, M. E. (2003) *J. Biol. Chem.* **278,** 51484–51493
15. Trinkle-Mulcahy, L., Ichikawa, K., Hartshorne, D. J., Siegman, M. J., and Butler, T. M. (1995) *J. Biol. Chem.* **270,** 18191–18194
16. MacDonald, J. A., Borman, M. A., Murani, A., Somlyo, A. V., Hartshorne, D. J., and Haystead, T. A. J. (2001) *Proc. Natl. Acad. Sci. U. S. A.* **98,** 2419–2424
17. Muranyi, A., MacDonald, J. A., Deng, J. T., Wilson, D. P., Haystead, T. A., Walsh, M. P., Erdodi, F., Kiss, E., Wu, Y., and Hartshorne, D. J. (2002) *Biochem. J.* **366,** 211–216
18. Muranyi, A., Zhang, R., Liu, F., Hirano, K., Ito, M., Epstein, H. F., and Hartshorne, D. J. (2001) *FEBS Lett.* **493,** 80–84
19. Broustas, C. G., Grammatikakis, N., Eto, M., Dent, P., Brautigan, D. L., and Kasid, U. (2002) *J. Biol. Chem.* **277,** 3053–3059
20. Borman, M. A., MacDonald, J. A., Muranyi, A., Hartshorne, D. J., and Haystead, T. A. (2002) *J. Biol. Chem.* **277,** 23441–23446
21. Kawai, T., Matsumoto, M., Takeda, K., Sanjo, H., and Akira, S. (1998) *Mol. Cell. Biol.* **18,** 1642–1651
22. Niiro, N., and Ikebe, M. (2001) *J. Biol. Chem.* **276,** 29567–29574
23. Ichiba, T., Hashimoto, Y., Nakaya, M., Kuraishi, Y., Tanaka, S., Kurata, T., Mochizuki, N., and Matsuda, M. (1999) *J. Biol. Chem.* **274,** 14376–14381
24. Grunstein, M., and Hogness, D. S. (1975) *Proc. Natl. Acad. Sci. U. S. A.* **72,** 3961–3965
25. Murata-Hori, M., Suizu, F., Iwasaki, T., Kikuchi, A., and Hosoya, H. (1999) *FEBS Lett.* **451,** 81–84
26. Uehata, M., Ishizaki, T., Satoh, H., Ono, T., Kawahara, T., Morishita, T., Tamakawa, H., Yamagami, K., Inui, J., Maekawa, M., and Narumiya, S. (1997) *Nature* **389,** 990–994
27. Kandabashi, T., Shimokawa, H., Mukai, Y., Matoba, T., Kunihiro, I., Morikawa, K., Ito, M., Takahashi, S., Kaibuchi, K., and Takeshita, A. (2002) *Arterioscler. Thromb. Vasc. Biol.* **22,** 243–248

ELSEVIER

Cardiovascular Research 64 (2004) 125–131

Cardiovascular Research

www.elsevier.com/locate/cardiores

Extraneuronal enzymatic degradation of myocardial interstitial norepinephrine in the ischemic region

Takafumi Fujii[a], Toji Yamazaki[a,*], Tsuyoshi Akiyama[a], Shunji Sano[b], Hidezo Mori[a]

[a] *Department of Cardiac Physiology, National Cardiovascular Center Research Institute, 5-7-1 Fujishiro-dai, Suita, Osaka 565-8565, Japan*
[b] *Department of Cardiovascular Surgery, Okayama University Medical School, Okayama 700-8558, Japan*

Received 19 March 2004; received in revised form 28 May 2004; accepted 14 June 2004
Available online 22 July 2004
Time for primary review 26 days

Abstract

Objective: Catechol *O*-methyltransferase (COMT) is believed to exert degradative action at high norepinephrine (NE) levels. Although COMT exists in cardiac tissues, the contribution of cardiac COMT activity to regional NE kinetics, particularly in ischemia-induced NE accumulation, remains unclear. We investigated the role of cardiac COMT in NE kinetics in the ischemic region. **Methods:** We implanted a microdialysis probe into the left ventricular myocardium of anesthetized rabbits and induced myocardial ischemia by 60-min coronary artery occlusion. We monitored myocardial interstitial levels of NE and its metabolites in the presence and absence of a COMT inhibitor. We intraperitoneally administered entacapone (10 mg/kg) 120 min before control sampling. **Results:** In control, entacapone increased interstitial dihydroxyphenylglycol (DHPG, intraneuronal NE metabolite by monoamine oxidase (MAO)) levels and decreased interstitial normetanephrine (NMN, extraneuronal NE metabolite by COMT) and 3-methoxy-4-hydroxyphenylglycol (MHPG, extraneuronal DHPG metabolite by COMT) levels, but did not change interstitial NE levels. Coronary occlusion increased NE levels to 165 ± 48 nM at 45–60 min of occlusion. This increase was accompanied by increases in DHPG and NMN levels (11.3 ± 1.1 and 9.3 ± 1.3 nM at 45–60 min of occlusion). Entacapone augmented the ischemia-induced NE and DHPG responses (333 ± 51 and 22.9 ± 2.4 nM at 45–60 min of occlusion). In contrast, the ischemia-induced NMN response was suppressed by entacapone (2.0 ± 0.4 nM at 45–60 min of occlusion). Reperfusion decreased interstitial NE levels and increased interstitial DHPG and NMN levels. Entacapone suppressed changes in NE and NMN levels, but augmented the increase in dialysate DHPG. **Conclusion:** Myocardial ischemia evoked increases in myocardial interstitial NE and NMN levels. COMT inhibition augmented the increase in NE (substrate of COMT) levels and suppressed the increase in NMN (metabolite by COMT) levels. In the ischemic heart, COMT contributes to the removal of accumulated NE in the myocardium.

Keywords: Adrenergic agonists; Autonomic nervous system; Ischemia; Reperfusion; Neurotransmitters

1. Introduction

It has been reported that myocardial ischemia evokes an excessive norepinephrine (NE) accumulation in the myocardial interstitial space [1,2]. Outward NE transport through the uptake$_1$ carrier has been proposed as an important mechanism responsible for this ischemia-induced NE accumulation [2–4]. The presence of such high NE levels in the myocardial interstitium may be involved in the progression of myocardial cell injury and a higher incidence of malignant arrhythmia [5,6].

In the non-ischemic heart, released NE is reclaimed by cardiac sympathetic nerve endings via the uptake$_1$ carrier and repackaged or metabolized to dihydroxyphenylglycol (DHPG) by monoamine oxidase (MAO). NE, which escapes the synapses to the myocardial interstitium, spills over into the bloodstream or is taken up by extraneuronal cells via the uptake$_2$ carrier and mainly degraded to NE metabolites by catechol *O*-methyltransferase (COMT) [6–9] (Fig. 1). In the ischemic heart, normal transport by the uptake$_1$ carrier is impaired and NE spills over into the bloodstream, which is decreased due to the reduction of myocardial blood flow [1]. Therefore, extraneuronal enzymatic degradation may be the only mechanism that decreases myocardial interstitial NE. Little information, however, is available on the extraneuronal NE degradation by COMT in the ischemic region [10,11].

* Corresponding author. Tel.: +81-6-6833-5012x2380; fax: +81-6-6872-8092.
E-mail address: yamazaki@ri.ncvc.go.jp (T. Yamazaki).

0008-6363/$ - see front matter © 2004 European Society of Cardiology. Published by Elsevier B.V. All rights reserved.
doi:10.1016/j.cardiores.2004.06.011

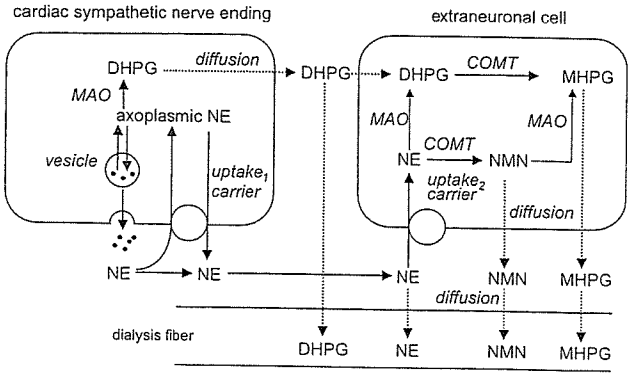

Fig. 1. Schema of putative factors affecting norepinephrine (NE) degradation in the cardiac sympathetic nerve ending and the extraneuronal cell. COMT, catechol *O*-methyltransferase; DHPG, dihydroxyphenylglycol; MAO, monoamine oxidase; NMN, normetanephrine; MHPG, 3-methoxy-4-hydroxyphenylglycol.

Until now, available methodology for examination of organ-specific NE degradation has been limited to the assessment of radiolabelled-catecholamine kinetics [12]. Previously, using the dialysis technique in the in vivo heart, we demonstrated that coronary occlusion evokes a marked increase of myocardial interstitial NE levels in the ischemic region [1,2,4] and that outward NE transport through the uptake$_1$ carrier is involved in this NE efflux [2–4]. Moreover, we recently reported that the dialysis technique makes it possible to simultaneously monitor interstitial levels of NE and extraneuronal metabolites in the rabbit skeletal muscle [13]. Therefore, we consider it possible to elucidate extraneuronal NE metabolism and the role of COMT in its metabolism in the ischemic region. In the present study, we applied the dialysis technique to the heart of anesthetized rabbits and investigated myocardial interstitial levels of NE and its extraneuronal metabolites during coronary occlusion and reperfusion and examined the effect of COMT blockade on myocardial interstitial levels of NE and its metabolites.

2. Methods

2.1. Animal preparation

The investigation conformed with the Guide for the Care and Use of Laboratory Animals published by the US National Institutes of Health (NIH Publication No. 85-23, revised 1996). Adult male Japanese white rabbits (2.5–3.2 kg) were anesthetized with pentobarbital sodium (30–35 mg/kg iv). The level of anesthesia was maintained with a continuous intravenous infusion of pentobarbital sodium (1–2 mg/kg/h). The rabbits were intubated and ventilated with room air mixed with oxygen. Body temperature was maintained at around 38 °C with a heating pad and lamp. Heart rate, arterial pressure, and electrocardiogram were monitored and recorded continuously. Heparin sodium (200 IU/kg) was first administered intravenously and then maintained with a continuous infusion (5–10 IU/kg/h) to prevent blood coagulation. With the animal in the lateral position, the fifth or sixth rib on the left side was partially removed to expose the heart. A small incision was made in the pericardium, and the dialysis probe was implanted in the region perfused by the left circumflex coronary artery (LCX) of the left ventricular wall. A snare was placed around the main branch of LCX to act as the occluder for later coronary occlusion. To ensure that the sampling area was in the ischemic region, we examined the color and motion of the ventricular wall during a brief occlusion and confirmed that the dialysis probe was correctly located. To avoid a preconditioning effect, the duration of occlusion was limited to within seconds.

2.2. Dialysis technique

Materials suitable for cardiac dialysis probes have been described in detail elsewhere [14]. Briefly, we designed a handmade long transverse dialysis probe. One end of a polyethylene tube (25-cm length, 0.5 mm OD, and 0.2 mm ID) was dilated with a 27-gauge needle (0.4 mm OD). Each end of the dialysis fiber (8-mm length, 0.31 mm OD, and 0.20 mm ID; PAN-1200 50 000 molecular weight cutoff, Asahi Chemical Japan) was inserted into the polyethylene tube and glued. We used a fine guiding needle (30-mm length, 0.51 mm OD, and 0.25 mm ID) for implantation of the dialysis probes. We connected a guiding needle to a dialysis probe with a stainless rod (5-mm length and 0.25 mm OD). At perfusion speed of 2 μl/min, in vitro recovery rates of NE, DHPG, normetanephrine (NMN), and 3-methoxy-4-hydroxyphenylglycol (MHPG) were 46 ± 8%, 48 ± 1%, 33 ± 3%, and 46 ± 2%, respectively (number of dialysis probes = 3) [15].

Dialysis probes were perfused with Ringer's solution at a speed of 2 μl/min using a microinjection pump (Carnegie Medicine CMA/100). Ringer's solution consisted of (in mM) 147.0 NaCl, 4.0 KCl, 2.25 $CaCl_2$. Sampling periods were 30 min (1 sampling volume = 60 μl) in control and 15 min (1 sampling volume = 30 μl) during occlusion and reperfusion. Each sample was collected in a microtube containing 3 μl of 0.1 N HCl to prevent amine oxidation. Based on the results of our previous study [1,2], we commenced the protocol followed by a stabilization period of 2 h. Taking into consideration the dead space between the dialysis fiber and sample tube, we sampled the dialysate.

Dialysate NE, DHPG, NMN, and MHPG concentrations were measured as indices of myocardial interstitial NE, DHPG, NMN, and MHPG levels. Furthermore, dialysate NE and DHPG were used as indices of COMT substrate, and dialysate NMN and MHPG as indices of COMT production. We used three distinct systems of high-performance liquid chromatography (HPLC) with electrochemical detection for the highly sensitive measurements: one for NE, one for DHPG, and one for NMN and MHPG measurement [16–18]. The mobile phase consisted of 1-octane-sulfonic acid sodium salt in phosphate buffer and methanol. In each HPLC system, the concentration of each component and the reference voltage were adjusted to the optimum condition. One-

third each of the dialysate sample was used for the measurement of NE, DHPG, and NMN and MHPG. Dialysate NE concentration was measured by the first HPLC after removing interfering compounds by the alumina procedure [14,16]. Dialysate DHPG concentration was measured by direct injection into the second HPLC [17]. Dialysate NMN and MHPG concentrations were measured by direct injection into the third HPLC [18]. The detection limits of NE, DHPG, NMN, and MHPG were 0.2, 0.2, 1, and 0.9 pg/injection.

2.3. Experimental protocols

After control sampling, we occluded the main branch of LCX for 60 min and then released the occluder. We continuously sampled dialysate from the ischemic region during 60 min of coronary occlusion and 15 min of reperfusion.

2.3.1. Vehicle group (n=8)

We administered saline intraperitoneally as vehicle 120 min before control sampling. After control sampling, we observed the time course of dialysate NE, DHPG, NMN, and MHPG levels from the ischemic region during 60 min of coronary occlusion and 15 min of reperfusion.

2.3.2. Entacapone group (n=8)

To elucidate role of COMT in the ischemia-induced changes in myocardial interstitial NE and its metabolites, we observed the effect of COMT inhibitor on dialysate NE, DHPG, NMN, and MHPG levels in the ischemic region. We administered intraperitoneally a COMT inhibitor entacapone (10 mg/kg; Orion Parma, Espoo, Finland) 120 min before control sampling. Entacapone was dissolved in phosphate-buffered saline, the pH of the solution was adjusted to 7.4. The route and dose of entacapone were selected to cause the full inhibition of soluble COMT in tissue [19]. After control sampling, we observed the time course of dialysate NE, DHPG, NMN, and MHPG levels with a similar protocol to that used in the vehicle group.

At the end of each experiment, the rabbits were killed with an overdose of pentobarbital sodium, and the implant regions were checked to confirm that the dialysis probes had been implanted within the cardiac muscle.

2.4. Statistical analysis

Hemodynamic and dialysate NE, DHPG, MHPG, and NMN responses to coronary occlusion in the presence and absence of COMT inhibitor were statistically analyzed by two-way analysis of variance with repeated measures on one factor [20]. When a statistically significant effect of coronary occlusion was detected as a whole, the Newman–Keuls test was applied to determine which mean values differed significantly from each other. When statistically significant effect of the COMT inhibitor was detected, the Newman–Keuls test was applied to determine which periods differed significantly between the vehicle and entacapone groups. Statistical significance was defined as $P<0.05$. Values are presented as means ± SE.

3. Results

3.1. Time course of heart rate and arterial pressure

The time course of heart rate and mean arterial pressure is shown in Table 1. In the vehicle group, heart rate decreased after 15 min of occlusion, whereas in the entacapone group, heart rate increased after 30 min of occlusion. There was, however, no significant difference in heart rate between groups.

Coronary occlusion significantly decreased mean arterial pressure in both groups. In the entacapone group, mean arterial pressure was higher than those in the vehicle group at each sampling point, while changes in mean arterial pressure were similar to those in the vehicle group.

3.2. Dialysate NE levels in the ischemic region

Coronary occlusion significantly altered dialysate NE levels (Fig. 2). In the vehicle group, dialysate NE levels were 0.39 ± 0.07 nM in the control and increased after coronary occlusion. During 60 min of coronary occlusion, dialysate NE levels markedly increased and reached 165 ± 48 nM at 45–60 min of occlusion. After reperfusion, dialysate NE levels decreased to 62 ± 40 nM, although their

Table 1
Time course of heart rate and mean arterial pressure during coronary occlusion and reperfusion

	Control	Coronary occlusion (min)				Reperfusion (min)
		15	30	45	60	15
Heart rate (bpm)						
Vehicle group ($n=8$)	252 ± 6	236 ± 7*	238 ± 7*	239 ± 6*	237 ± 6*	238 ± 6*
Entacapone group ($n=8$)	246 ± 8	246 ± 8	251 ± 9*	253 ± 7*	253 ± 8*	251 ± 9
Mean arterial pressure (mm Hg)						
Vehicle group ($n=8$)	83 ± 3	71 ± 4*	75 ± 3*	76 ± 3*	78 ± 2*	76 ± 3*
Entacapone group ($n=8$)	99 ± 4†	85 ± 4*,†	88 ± 5*,†	88 ± 4*,†	88 ± 4*,†	86 ± 4*,†

Values are means ± SE.
* $P<0.05$ vs. control value.
† $P<0.05$ vs. concurrent value of vehicle group.

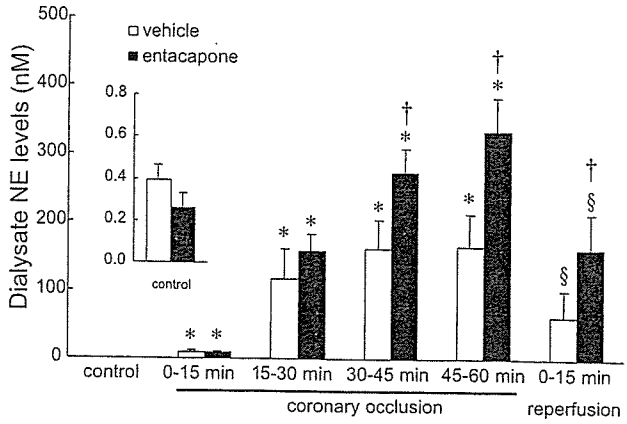

Fig. 2. Dialysate norepinephrine (NE) levels in the ischemic region. Values are means ± SE. *$P<0.05$ vs. control value, §$P<0.05$ vs. value at 45–60 min of occlusion, †$P<0.05$ vs. concurrent value of vehicle group.

levels were higher than those in the control. In the presence of entacapone, dialysate NE levels also markedly increased and reached 333 ± 51 nM at 45–60 min of occlusion. These increases in dialysate NE levels after 30 min of coronary occlusion were significantly enhanced by entacapone whereas entacapone did not change dialysate NE levels in the control (0.26 ± 0.07 nM). After reperfusion, dialysate NE levels decreased but remained higher than those in the vehicle group.

3.3. Dialysate DHPG levels in the ischemic region

Coronary occlusion significantly altered dialysate DHPG levels (Fig. 3). In the vehicle group, dialysate DHPG levels were 6.5 ± 0.5 nM in the control and did not change within 30 min of coronary occlusion. After 30 min of occlusion, dialysate DHPG levels gradually increased and reached 11.3 ± 1.1 nM at 45–60 min of occlusion. After reperfusion, dialysate DHPG levels further increased to 29.5 ± 2.6 nM. In the presence of entacapone, dialysate DHPG levels gradually increased during the ischemia and reached 22.9 ± 2.4 nM at 45–60 min of occlusion. After reperfusion, dialysate DHPG levels further increased to 52.6 ± 8.4 nM. In the presence of entacapone, dialysate DHPG levels in the control (9.9 ± 0.8 nM) and after reperfusion were higher than those in the vehicle group.

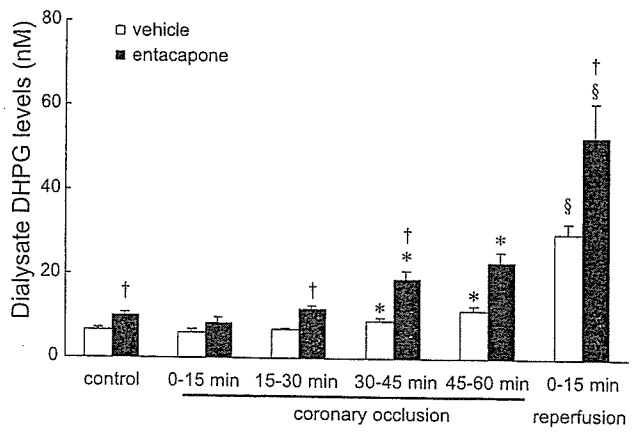

Fig. 3. Dialysate dihydroxyphenylglycol (DHPG) levels in the ischemic region. Values are means ± SE. *$P<0.05$ vs. control value, §$P<0.05$ vs. value at 45–60 min of occlusion, †$P<0.05$ vs. concurrent value of vehicle group.

3.4. Dialysate NMN levels in the ischemic region

Coronary occlusion significantly altered dialysate NMN levels (Fig. 4). In the vehicle group, dialysate NMN levels were 2.9 ± 0.4 nM in the control and increased after 30 min of occlusion and reached 9.3 ± 1.3 nM at 45–60 min of occlusion. After reperfusion, dialysate NMN levels further increased (11.9 ± 2.0 nM). Entacapone decreased dialysate NMN levels in the control to undetectable levels. Then dialysate NMN levels increased after 30 min of occlusion and reached 2.0 ± 0.4 nM at 45–60 min of occlusion. After reperfusion, dialysate NMN levels further increased to 4.1 ± 0.8 nM. Their NMN levels were lower than those in the vehicle group at each sampling point before, during, and after coronary occlusion.

3.5. Dialysate MHPG levels in the ischemic region

Coronary occlusion significantly altered dialysate MHPG levels (Fig. 5). In the vehicle group, dialysate MHPG levels were 3.9 ± 0.3 nM in the control. Dialysate MHPG levels transiently decreased 15–30 min after occlusion (3.6 ± 0.4 nM), but recovered after 30 min of occlusion. After reperfusion, dialysate MHPG levels increased to 5.5 ± 0.3 nM. Entacapone substantially decreased dialysate MHPG levels in the control (1.5 ± 0.4 nM). In the presence of entacapone, dialysate MHPG levels further decreased during occlusion and reached 0.6 ± 0.2 nM at 30–45 min of occlusion. After reperfusion, dialysate MHPG levels increased to 2.3 ± 0.5 nM. Their MHPG levels were lower than those in the

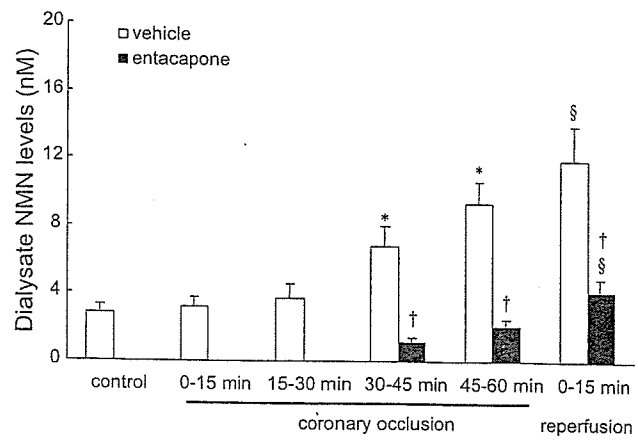

Fig. 4. Dialysate normetanephrine (NMN) levels in the ischemic region. Values are means ± SE. *$P<0.05$ vs. control value, §$P<0.05$ vs. value at 45–60 min of occlusion, †$P<0.05$ vs. concurrent value of vehicle group.

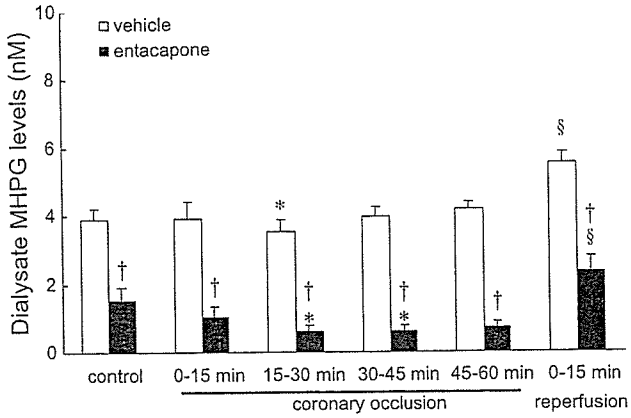

Fig. 5. Dialysate 3-methoxy-4-hydroxyphenylglycol (MHPG) levels in the ischemic region. Values are means ± SE. *$P<0.05$ vs. control value, §$P<0.05$ vs. value at 45–60 min of occlusion, †$P<0.05$ vs. concurrent value of vehicle group.

vehicle group at each sampling point before, during, and after coronary occlusion.

4. Discussion

Using the dialysis technique in the in vivo rabbit heart, we observed myocardial interstitial levels of NE and its neuronal and extraneuronal metabolites in the ischemic region and examined the contribution of extraneuronal NE degradation by COMT to myocardial interstitial NE levels. Our data demonstrate that COMT plays an important role in NE metabolism during 60 min of coronary occlusion and reperfusion.

4.1. Myocardial interstitial NE and its metabolites under control conditions

The administration of entacapone did not alter myocardial interstitial NE levels in the control. Degradation of NE by COMT may play a minor role in the changes in myocardial NE levels [21]. In general, NE that is taken up by cardiac sympathetic nerve endings is repackaged or metabolized to DHPG by MAO. On the other hand, NE that is taken up via extraneuronal NE transport systems by extraneuronal cells is metabolized to NMN or MHPG by COMT [7–10,22,23] (Fig. 1). In the present study, entacapone increased DHPG in the myocardial interstitium but did not alter myocardial interstitial NE levels in the control. Myocardial interstitial levels of DHPG were about 16-fold higher than those of NE and about 2- to 3-fold higher than those of NMN in the control. Therefore, under physiological conditions, released NE could be largely taken up by cardiac sympathetic nerve endings via the $uptake_1$ carrier and transferred into stored vesicle or metabolized to DHPG by MAO. A smaller percentage of released NE, which escapes the synapses, is taken up by extraneuronal cells via the $uptake_2$ carrier and is metabolized to NMN by COMT. Compared with MAO, COMT could play a minor role on the degradation of released NE in the control.

After entacapone administration, increases in myocardial interstitial DHPG accompanied decreases in myocardial interstitial MHPG levels in the control. These metabolites of NE penetrate the cell membrane by diffusion [24]. Their values serve as indices of the neuronal and extraneuronal NE metabolism. COMT blockade suppressed the degradation of DHPG to MHPG. Therefore, the decrease in MHPG levels and increase in interstitial DHPG levels could be ascribed to inhibition of COMT by entacapone. In rabbit heart, we confirmed the existence of COMT activity with the main substrate of COMT being DHPG rather than NE.

4.2. Myocardial interstitial NE and its metabolites during coronary occlusion

Myocardial interstitial NE levels markedly increased after 15 min of occlusion. In this phase, outward transport of NE via the $uptake_1$ carrier takes place from cardiac sympathetic nerve endings [2,3]. The marked increase in myocardial interstitial NE could be due to this non-exocytotic NE release and inhibition of neuronal reuptake via the $uptake_1$ carrier [2–4].

Entacapone augmented increases in myocardial interstitial NE levels after 30 min of coronary occlusion. This result indicates that COMT contributes to the degradation of myocardial interstitial NE in this phase. Neuronal reuptake via the normal mode of $uptake_1$ is dependent on the sodium gradient between the intra- and extraneuronal space [25]. Neuronal degradation of released NE via neuronal uptake cannot be expected in this phase because of a reduced sodium gradient [3,25]. Moreover, NE spillover into the bloodstream is decreased due to reduced myocardial blood flow [1]. On the other hand, extraneuronal NE uptake operates independently of the sodium gradient [26]. Burgdorf et al. [27] demonstrated that the extraneuronal monoamine transporter is activated during metabolic distress such as low flow ischemia. Previous investigations with similar preparations suggested that ketamine augments ischemia-induced NE accumulation by inhibition of extraneuronal uptake [28,29]. We consider that substantial NE in the myocardial interstitium is taken up alternatively by extraneuronal cells via the $uptake_2$ carrier and is metabolized to NMN by COMT in this phase. Thus, COMT activity plays an important physiological role in NE degradation in the ischemic period.

Myocardial interstitial NMN levels increased after 30 min of occlusion. Entacapone decreased basal myocardial interstitial NMN levels and suppressed the ischemia-induced increase in myocardial interstitial NMN levels. This suppression is consistent with the finding that COMT contributes to the degradation of myocardial interstitial NE via extraneuronal NE uptake. Furthermore, even in the presence of entacapone, myocardial interstitial NMN levels increased after 30 min of occlusion. An increase in interstitial NE levels may overcome the inhibition of COMT by

entacapone. Although COMT could play a minor role in the degradation of released NE in the control, a substantial increase in myocardial NE may cause the high affinity of the extraneuronal COMT system. In the control period, an extraneuronal COMT system may contribute to DHPG degradation, whereas in the ischemic period, both neuronal NE uptake and MAO activities may be suppressed by ischemia and alternatively the extraneuronal COMT system may promote NE degradation based on the fact that the myocardial interstitial NE levels in the ischemic period were 10-fold higher than those of DHPG. Therefore, we consider that increases in myocardial interstitial NE levels shift the main substrate of COMT from DHPG to NE.

The relationship between DHPG and MHPG supports our interpretation. In the control, entacapone increased myocardial interstitial DHPG levels and decreased myocardial interstitial MHPG levels. In contrast, in the ischemic period, increases in myocardial interstitial DHPG levels were not associated with increases in myocardial MHPG levels, but increases in myocardial NE levels accompanied increases in myocardial NMN. Thus, both DHPG and NE are metabolized by the extraneuronal COMT system, but the amount of NMN and MHPG may be dependent on the concentration of their substrate. Thus, there was a clear difference in the main metabolite by COMT between the non-ischemic and ischemic periods. The main metabolite by COMT was NMN rather than MHPG in the latter [30]. These results are limited to ischemia within 60 min because prolonged ischemia accompanies the structural membrane defects, and other mechanisms for NE release and degradation may be involved [31].

4.3. Myocardial interstitial NE and its metabolites after reperfusion

Myocardial interstitial NE levels decreased after reperfusion although they were higher than those in control. On the other hand, myocardial interstitial DHPG levels increased after reperfusion. The uptake$_1$ carrier resumes normal transport function after reperfusion [2,4]. The inward NE transport via the uptake$_1$ carrier could contribute to the decrease in myocardial interstitial NE levels. The increase in axoplasmic NE by uptake and the recovery of MAO activity could increase myocardial interstitial DHPG levels [2]. Thus, neuronal degradation by MAO contributes to decreasing myocardial interstitial NE after reperfusion.

Reperfusion caused a decrease in myocardial interstitial NE levels and an increase in myocardial NMN levels, both of which changes were suppressed by administration of entacapone. During the early reperfusion period, COMT activity promotes the degradation of NE. Myocardial interstitial NE levels were higher than those in the control. Therefore, during the ischemic and reperfusion periods, these higher NE levels in myocardial interstitium may serve as an effective substrate of COMT for NE degradation via extraneuronal NE uptake.

During the reperfusion period, increases in myocardial interstitial DHPG accompanied increases in myocardial interstitial MHPG levels. Furthermore, administration of entacapone suppressed both of these changes. Myocardial interstitial DHPG levels were similar to myocardial interstitial NE levels. These data suggest that COMT activity promotes the degradation of DHPG. Alternatively, higher NE level in myocardial interstitium may produce MHPG via COMT activity. Recently, we demonstrated in rabbit skeletal muscle that local administration of higher NE increased dialysate NMN but not MHPG levels, whereas local administration of higher DHPG increased dialysate MHPG levels [19]. Therefore, higher NE and DHPG levels serve as the substrate of COMT and independently yield NMN and MHPG during the reperfusion period. Thus, COMT activity plays an important physiological role in the reperfusion period.

4.4. Methodological considerations

In the presence of a high concentration of entacapone, mean arterial pressure was higher than that in the vehicle group at each sampling point before, during, and after coronary occlusion, but changes in mean arterial pressure were similar to those in the vehicle group. In the previous and present studies, intraperitoneal administration of entacapone did not alter control dialysate NE levels from skeletal muscle and myocardium [19]. In humans, entacapone did not alter plasma catecholamine levels or hemodynamics at rest or during exercise [32]. The influence of entacapone on pressure-regulating peptides remains unclear. An increase in mean arterial blood pressure might decrease dialysate NE levels through a baroreflex mechanism. Furthermore, baroreflex-independent and non-exocytotic NE efflux leads to high NE levels in the myocardial interstitium of ischemic regions, making it unlikely that hemodynamic change contributes to the removal of accumulated NE during myocardial ischemia.

Two major classes of COMT have been defined on the basis of their location: a soluble, cytosolic form and a membrane-bound form [33]. Entacapone inhibits both classes of COMT. The soluble, cytosolic form is generally assumed to be the predominant form of the enzyme. The membrane-bound form has been suggested to be responsible for O-methylation at low and physiologically relevant concentrations of the catecholamine neurotransmitters, whereas the soluble, cytosolic form predominates under conditions that lead to saturation of the membrane-bound form [33]. In the present study, myocardial interstitial norepinephrine levels reached 100–1000 times the normal plasma concentrations after 15 min of occlusion. Thus, a soluble, cytosolic form could contribute to the observed decrease in myocardial interstitial NE levels in the ischemic region.

5. Conclusion

Under physiological condition, extraneuronal enzymatic degradation by COMT plays a minor role on the inactivation

of myocardial interstitial NE. Under ischemic conditions, however, myocardial interstitial NE levels are markedly increased by ischemia. Normal transport by the uptake$_1$ carrier is impaired and NE spillover into the bloodstream is decreased due to the reduction of myocardial blood flow, but extraneuronal enzymatic degradation by COMT contributes to the decrease in myocardial interstitial NE levels in the ischemic region.

Acknowledgements

This work was supported by Grants-in-Aid for scientific research (15590787) from the Ministry of Education, Culture, Sports, Science and Technology; the Research Grants for Cardiovascular Disease (H13C-1) from the Ministry of Health, Labor and Welfare. The authors thank Orion-Pharma (Espoo, Finland) for the supply of entacapone.

References

[1] Akiyama T, Yamazaki T, Ninomiya I. Differential regional responses of myocardial interstitial noradrenaline levels to coronary occlusion. Cardiovasc Res 1993;27:817–22.
[2] Akiyama T, Yamazaki T. Myocardial interstitial norepinephrine and dihydroxyphenylglycol levels during ischemia and reperfusion. Cardiovasc Res 2001;49:78–85.
[3] Schömig A, Dart AM, Dietz R, Mayer E, Kübler W. Release of endogenous catecholamines in the ischemic myocardium of the rat. Part A: locally mediated release. Circ Res 1984;55:689–701.
[4] Shindo T, Akiyama T, Yamazaki T, Ninomiya I. Regional myocardial interstitial norepinephrine kinetics during coronary occlusion and reperfusion. Am J Physiol 1996;270:H245–51.
[5] Penny WJ. The deleterious effects of myocardial catecholamines on cellular electrophysiology and arrhythmias during ischaemia and reperfusion. Eur Heart J 1984;5:960–73.
[6] Waldenström AP, Hjalmarson AC, Thornell L. A possible role of noradrenaline in the development of myocardial infarction. Am Heart J 1978;95:43–51.
[7] Boulton AA, Eisenhofer G. Catecholamine metabolism. From molecular understanding to clinical diagnosis and treatment. Adv Pharmacol 1998;42:273–92.
[8] Grohmann M, Trendelenburg U. The substrate specificity of uptake2 in the rat heart. Naunyn Schmiedebergs Arch Pharmacol 1984;328: 164–73.
[9] Obst OO, Rose H, Kammermeier H. Characterization of catecholamine uptake2 in isolated cardiac myocytes. Mol Cell Biochem 1996;163–164:181–3.
[10] Inoue M, Hifumi K, Kurahashi K, Fujiwara M. Impairment of the extraneuronal O-metylating system of isoproterenol by stop-flow ischemia in the perfused rat heart. J Pharmacol Exp Ther 1987;242: 1086–9.
[11] Carlsson L, Abrahamsson T, Almgren O. Release of noradrenaline in myocardial ischemia-importance of local inactivation by neuronal and extraneuronal mechanisms. J Cardiovasc Pharmacol 1986;8:543–53.
[12] Goldstein DS, Katzper M, Linares O, Kopin I. Kinetic model from the fate of 6-[^{18}F]fluorodopamine in the human heart: a novel means to examine cardiac sympathetic neuronal function. Naunyn Schmiedebergs Arch Pharmacol 2002;365:38–49.
[13] Tokunaga N, Yamazaki T, Akiyama T, Sano S, Mori H. In vivo monitoring of norepinephrine and its metabolites in skeletal muscle. Neurochem Int 2003;43:573–80.
[14] Akiyama T, Yamazaki T, Ninomiya I. In vivo monitoring of myocardial interstitial norepinephrine by dialysis technique. Am J Physiol 1991;261:H1643–7.
[15] Le Quellec A, Dupin S, Genissel P, Saivin S, Marchand B, Houin G. Microdialysis probe calibration: gradient and tissue dependent changes in no net flux and reverse dialysis methods. J Pharmacol Toxicol Methods 1995;33:11–6.
[16] Yamazaki T, Akiyama T, Shindo T. Routine high-performance liquid chromatographic determination of myocardial interstitial norepinephrine. J Chromatogr B, Biomed Sci Appl 1995;670:328–31.
[17] Takauchi Y, Kitagawa H, Kawada T, Akiyama T, Yamazaki T. High-performance liquid chromatographic determination of myocardial interstitial dihydroxyphenylglycol. J Chromatogr B, Biomed Sci Appl 1997;693:218–21.
[18] Tokunaga N, Yamazaki T, Akiyama T, Mori H. Detection of 3-methoxy-4-hydroxyphenylglycol in rabbit skeletal muscle microdialysate. J Chromatogr B, Biomed Sci Appl 2003;798:163–6.
[19] Fujii T, Yamazaki T, Akiyama T, Sano S, Mori H. In vivo assessment of catechol *O*-methyltransferase activity in rabbit skeletal muscle. Auton Neurosci 2004;111:140–3.
[20] Winer BJ. Statistical principles in experimental design. 2nd ed. New York: McGraw-Hill; 1971.
[21] Trendelenburg U. The extraneuronal uptake and metabolism of catecholamines in the heart. In: Paton DM, editor. The mechanism of neuronal and extraneuronal transport of catecholamines. 1st ed. New York: Raven Press; 1976. p. 259–80.
[22] Eisenhofer G, Pecorella W, Pacak K, Hooper D, Kopin I. The neuronal and extraneuronal origins of plasma 3-methoxy-4-hydroxyphenylglycol in rats. J Auton Nerv Syst 1994;50:93–107.
[23] Friedgen B, Wolfel R, Russ H, Schömig E, Graefe KH. The role of extraneuronal amine transport systems for the removal of extracellular catecholamine in the rabbit. Naunyn Schmiedebergs Arch Pharmacol 1996;354:275–86.
[24] Goldstein D, Eisenhofer G, Stull R, Joan Folio C, Kaiser HR, Kopin IJ. Plasma dihydroxyphenylgylcol and intraneuronal disposition of norepinephrine in humans. J Clin Invest 1988;81:213–20.
[25] Schömig A, Kurz T, Richardt G, Schömig E. Neuronal sodium homeostasis and axoplasmic amine concentration determine calcium-independent noradrenaline release in normoxic and ischemic rat heart. Circ Res 1988;63:214–26.
[26] Schömig E, Russ H, Staudt K, Martel F, Gliese M, Gründemann D. The extraneuronal monoamine transporter exists in human central nervous system glia. Adv Pharmacol 1998;42:356–9.
[27] Burgdorf C, Dendorfer A, Kurz T, Schömig E, Stolting I, Schutte F, et al. Role of neuronal KATP channels and extraneuronal monoamine transporter on norepinephrine overflow in a model of myocardial low flow ischemia. J Pharmacol Exp Ther 2004;309:42–8.
[28] Kitagawa H, Yamazaki T, Akiyama T, Yahagi N, Kawada T, Mori H, et al. Modulatory effects of ketamine on catecholamine efflux from in vivo cardiac sympathetic nerve endings in cats. Neurosci Lett 2002;324:232–6.
[29] Lundy PM, Frew R. Ketamine potentiates catecholamine responses of vascular smooth muscle by inhibition of extraneuronal uptake. Can J Physiol Pharmacol 1981;59:520–7.
[30] Eisenhofer G. Plasma normetanephrine for examination of extraneuronal uptake and metabolism of noradrenaline in rats. Naunyn Schmiedebergs Arch Pharmacol 1994;349:259–69.
[31] Schömig A. Catecholamine in myocardial ischemia. Systemic and cardiac release. Circulation 1990;82(3 Suppl):II13–22.
[32] Illi A, Sundberg S, Koulu M, Scheinin M, Heinavaara S, Gordin A. COMT inhibition by high-dose entacapone does not affect hemodynamics but changes catecholamine metabolism in healthy volunteers at rest and during exercise. Int J Clin Pharmacol Ther 1994;32:582–8.
[33] Männistö PT, Kaakkola S. Catechol-*O*-methyltransferase (COMT): biochemistry, molecular biology, pharmacology, and clinical efficacy of the new selective COMT inhibitors. Pharmacol Rev 1999;51: 593–628.

ELSEVIER

Autonomic Neuroscience: Basic and Clinical 111 (2004) 140–143

AUTONOMIC NEUROSCIENCE: Basic & Clinical

www.elsevier.com/locate/autneu

Short communication

In vivo assessment of catechol *O*-methyltransferase activity in rabbit skeletal muscle

Takafumi Fujii[a], Toji Yamazaki[a,*], Tsuyoshi Akiyama[a], Shunji Sano[b], Hidezo Mori[a]

[a] *Department of Cardiac Physiology, National Cardiovascular Center Research Institute, 5-7-1, Fujishirodai, Suita, Osaka 565-8565, Japan*
[b] *Department of Cardiovascular Surgery, Okayama University Medical School, Okayama 700-8558, Japan*

Received 25 December 2003; received in revised form 23 January 2004; accepted 9 February 2004

Abstract

With the use of microdialysis technique in the anesthetized rabbit, we examined the catechol *O*-methyltransferase (COMT) activity at the skeletal muscle interstitium. We implanted a dialysis probe into the adductor muscle, and monitored dialysate catecholamines and their metabolites with chromatogram-electrochemical detection. Administration of COMT inhibitor (entacapone) decreased dialysate 3-methoxy 4-hydroxyphenylglycol (MHPG) levels. Local administration of dihydroxyphenylglycol induced increases in dialysate MHPG levels. These increases in dialysate MHPG levels were suppressed by the addition of entacapone. The concentration of MHPG in the skeletal muscle dialysate corresponded to the COMT activity in the skeletal muscle. Furthermore, local administration of norepinephrine or epinephrine increased normetanephrine or metanephrine levels in dialysate but not MHPG levels. Skeletal muscle microdialysis with local administration of catecholamine offers a new method for in vivo assessment of regional COMT activity.

Keywords: Catecholamine; Catechol *O*-methyltransferase; Entacapone; Microdialysis; Skeletal muscle

Catechol *O*-methyltransferase (COMT) exerts a critical action on the inactivation of catecholamrines and catecholestrogens (Boulton and Eisenhofer, 1998). COMT enzyme exists in almost all mammalian tissues and organs (Karhunen et al., 1994; Männistö and Kaakkola, 1999). The wide distribution of COMT in different tissues suggests an important physiological role for COMT activity. In vitro COMT activity has been widely assessed in various tissues (Männistö and Kaakkola, 1999; Tsunoda et al., 2002), while in vivo COMT activity has been assessed only in erythrocyte (Toumainen et al., 1996). To determine whether COMT activity is involved in cardiovascular regulation, we need information about in vivo COMT activity in organs and tissues.

A sophisticated technique using radiotracers has been employed for spillover of organ specific metabolite formed by COMT activity (3-methoxy 4-hydroxyphenylglycol, MHPG) (Lambert et al., 1995). This study suggested that majority of MHPG in plasma was derived from skeletal muscle, with the exception of central nervous system. Dispersed organs, such as skeletal muscle, have a thin and diffuse sympathetic innervation, but skeletal muscle is one candidate suitable for investigating regional MHPG production (Tokunaga et al., 2003a,b). This organ is suited to microdialysis probe implantation. Recently we have developed the skeletal muscle microdialysis for the monitoring of catecholamines and their metabolites. At the skeletal muscle, the small amounts of dialysate norepinephrine and its metabolites could be determined by microdialysis with electrochemical detection.

In the present study, we examined whether COMT blocker affected regional norepinephrine kinetics at the skeletal muscle interstitial spaces. With the use of dialysis technique, the dialysate was sampled from the skeletal muscle, and dialysate catecholamines and their metabolites levels were measured with liquid chromatography. Further, the study was designed to examine regional *O*-methylation products evoked by local administration of catecholamine and determine whether these data provide information about in vivo regional COMT activity.

Male Japanese white rabbits weighing 2.6–3.1 kg each were anesthetized with pentobarbital sodium (30–35 mg/kg,

* Corresponding author. Tel.: +81-6-6833-5012; fax: +81-6-6872-8092.
E-mail address: yamazaki@ri.ncvc.go.jp (T. Yamazaki).

1566-0702/$ - see front matter © 2004 Elsevier B.V. All rights reserved.
doi:10.1016/j.autneu.2004.02.001

i.v.). The level of anesthesia was maintained with a continuous intravenous infusion of pentobarbital sodium (1–2 mg/kg/h). After tracheotomy, the animals were ventilated with room air mixed with oxygen. Body temperature was maintained with a heated pad and lamp. All protocols were performed in accordance with the American Physiological Society guidelines for the use of animals. After a longitudinal skin incision was made in the left groin, the dialysis probes were implanted in the left adductor muscle with a fine guiding needle.

For skeletal muscle dialysis, we designed a transverse dialysis probe. The dialysis fiber (13 mm length, 0.31 mm O.D. and 0.2 mm I.D.; PAN-1200, 50,000 molecular mass cutoff, Asahi Chemical, Tokyo, Japan) was glued at both ends into a polyethylene tube (25 cm length, 0.5 mm O.D. and 0.2 mm I.D.) (Akiyama et al., 1991; Tokunaga et al., 2003a,b). The dialysis probe was perfused with Ringer solution at a speed of 10 μl/min using a microinjection pump (CMA 102, Carnegie Medicin, Stockholm, Sweden). Dialysate catecholamines and their metabolite concentrations were measured by high-performance liquid chromatography with electrochemical detection (Takauchi et al., 1997; Tokunaga et al., 2003a,b; Yamazaki et al., 1995).

Basal dialysate norepinephrine, dihydroxyphenylglycol (DHPG) and MHPG levels were presented in Table 1. Entacapone (COMT blocker) was intraperitoneally administered (10 mg/kg) (Illi et al., 1995; Scheinin et al., 1998). Administration of entacapone decreased the MHPG level of dialysate but increased the DHPG levels of dialysate. The dialysate norepinephrine levels were not affected by entacapone. These changes were preserved 2 h after administration of entacapone.

To examine regional COMT activity, we measured the formation of MHPG evoked by local administration of exogenous DHPG via dialysis probe. We determined doses of DHPG based on the dialysate DHPG concentration in the previous experiments (Akiyama and Yamazaki, 2001). Local administration of DHPG (25, 250 ng/ml) dose-dependently increased the MHPG levels of dialysate (Fig. 1). These increases in the MHPG levels were prevented by pretreatment with entacapone.

In this study, exogenous DHPG dose-dependently increased the MHPG levels of dialysate. Exogenous DHPG via the dialysis probe easily traversed the cell membrane and reached skeletal muscle (Goldstein et al., 1998). In contrast, entacapone significantly decreased the MHPG levels of dialysate. These data suggest that regional COMT activity corresponds to the production of dialysate MHPG levels. Furthermore, entacapone induced a decrease in the dialysate MHPG level accompanied by an increase in the dialysate DHPG but not norepinephrine level. Therefore we consider that regional DHPG is one possible substrate for MHPG production, and that the concentration of MHPG or MHPG/DHPG ratio in the skeletal muscle dialysate might correspond to the COMT activity in the skeletal muscle.

Table 1
Basal dialysate NE, DHPG, and MHPG levels in rabbit skeletal muscle

	Before entacapone	After entacapone
NE (pg/ml)	8±1	10±1
DHPG (pg/ml)	27±4	53±11*
MHPG (pg/ml)	198±12	147±18*

NE, norepinephrine; DHPG, dihydroxyphenylglycol; MHPG, 3-methoxy 4-hydroxyphenylglycol. Values are means±SE. n=5.
* P<0.05 vs. values before entacapone.

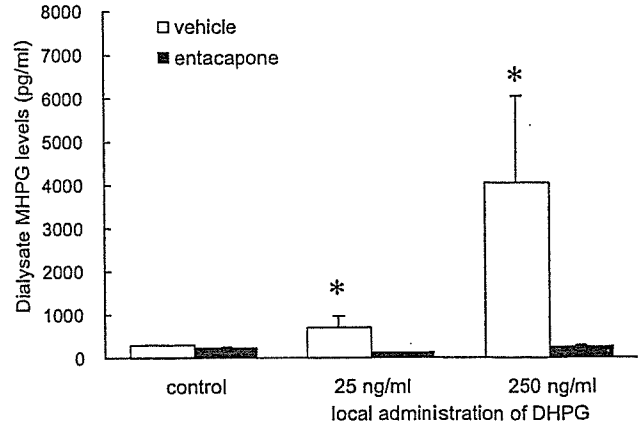

Fig. 1. Effects of exogenous dihydroxyphenylglycol (DHPG) infusion on the 3-methoxy 4-hydroxyphenylglycol (MHPG) production. Local administration of DHPG dose-dependently increased the MHPG levels of dialysate. These increases in the MHPG levels were prevented by pretreatment with entacapone. Values are means±SE (n=5). *P<0.05 vs. control.

Earlier studies suggested species and organ differences in extraneuronal uptake and COMT activity (Scheinin et al., 1998; Tsunoda et al., 2002). Extraneuronal norepinephrine uptake and COMT activity were well examined in rabbit heart with the findings suggesting that rabbit heart hardly metabolizes isoprenaline to methoxyprenaline (Lindmar and Löffelholz, 1974). Thus rabbit heart seems to have a very poorly developed extraneuronal system, including weak COMT activity, for the uptake and metabolism of catecholamines (Trendelenburg, 1978). On the other hand, rabbit aortic strips have a high capacity for COMT activity (Levin, 1974). From these and previous data (Tokunaga et al., 2003a,b), the ratio of MHPG/DHPG in myocardium and skeletal muscle were 1.0±0.2 and 7.9±1.3, respectively. Rabbit skeletal muscle seems to have a well-developed COMT activity. In the skeletal muscle sympathetic innervation was not dense, and the DHPG levels were less than that of heart (Tokunaga et al., 2003a,b). Therefore, other compounds or plasma DHPG might be involved in the regional formation of MHPG in the skeletal muscle.

MHPG is produced by extraneuronal *O*-methylation of DHPG formed intraneuronally from norepinephrine or by the extraneuronal combination of COMT and monoamine oxidase (MAO) on norepinephrine and epinephrine (Akiyama and Yamazaki, 2001; Eisenhofer et al., 1988). Therefore, MHPG is mainly yielded from DHPG, norepinephrine or epinephrine at the skeletal muscle. Furthermore,

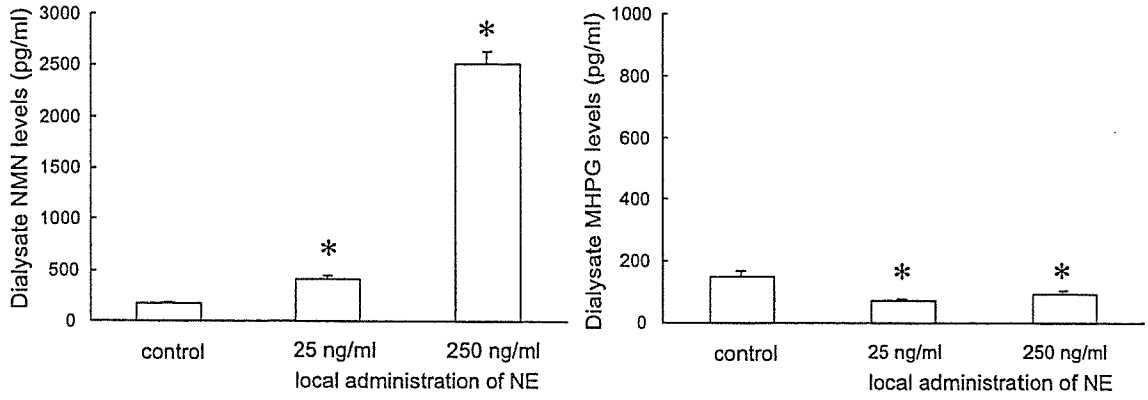

Fig. 2. Effects of exogenous norepinephrine (NE) infusion on the 3-methoxy 4-hydroxyphenylglycol (MHPG) and normetanephrine (NMN) production. Local administration of NE dose-dependently increased the NMN levels of dialysate but not MHPG levels. Values are means±SE (n=5). *P<0.05 vs. control.

O-methylation of catechol compounds includes MHPG, normetanephrine and metanephrine. We examined the relation between catecholamines and their metabolites. To compare norepinephrine and epinephrine with DHPG infusion, norepinephrine or epinephrine infusion with similar doses of DHPG was administered. Local administration of norepinephrine increased the normetanephrine levels of dialysate but not the MHPG levels (Fig. 2). Local administration of epinephrine increased the metanephrine levels of dialysate but not the MHPG levels (Fig. 3). Our data suggest that only DHPG is a possible substrate for MHPG production. Local administration of norepinephrine or epinephrine produced normetanephrine or metanephrine but not MHPG. Or rather, norepinephrine or epinephrine caused a decrease in the dialysate MHPG level. These data are consistent with data on the origins of plasma MHPG in rats, which indicated that most MHPG arises from *O*-methylation of the DHPG by intraneuronal deamination of norepinephrine (Eisenhofer et al., 1994).

Our data indicate that COMT exerts an important role on the degradation of cathecholamines in the skeletal muscular interstitium. Muscular catecholamines derive from circulating blood and surrounding sympathetic nerve systems (Tokunaga et al., 2003a,b). Therefore, COMT activity in the skeletal muscle may be related to regional or systemic sympathetic nerve activity. The relationship between regional COMT activity and sympathetic nerve activity remains to be further examined. Muscle sympathetic nerve activity is involved in the regulation of vascular tone and glucose metabolism in the skeletal muscle (Lundvall and Edfeldt, 1994; Spraul et al., 1994). Further studies concerning the physiological role of regional COMT activity on vascular or metabolic control are warranted.

To our knowledge, this is the first report on the in vivo assessment of COMT activity by direct measurement of dialysate MHPG, normetanephrine, and metanephrine obtained from skeletal muscle. Local administration of DHPG increased the MHPG levels of dialysate. These increases in MHPG were prevented by pretreatment with a COMT inhibitor. Therefore we consider that the concentration of MHPG in the skeletal muscle dialysate might correspond to the COMT activity in the skeletal muscle. Measurement of MHPG/DHPG ratio or MHPG formation evoked by DHPG infusion in skeletal muscle may be particularly appropriate for providing information about regional COMT activity. Thus skeletal muscle microdialysis with local administration of catecholamine offers a new method for in vivo assessment of regional COMT activity.

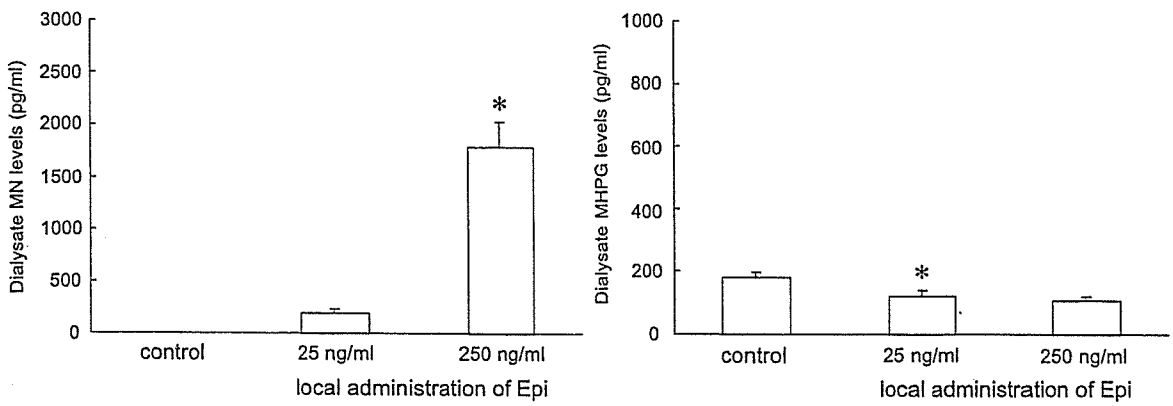

Fig. 3. Effects of exogenous epinephrine (Epi) infusion on the metanephrine (MN) and 3-methoxy 4-hydroxyphenylglycol (MHPG) production. Local administration of Epi increased the MN levels of dialysate but not MHPG levels. Values are means±SE (n=5). *P<0.05 vs. control.